Distributions of dissolved organic carbon and nitrogen in the western Okhotsk Sea and their effluxes to the North Pacific

Distributions of dissolved organic carbon and nitrogen in the western Okhotsk Sea and their effluxes to the North Pacific

Rumi Sohrin[*a, b], Kunimatsu Imanishi[a], Yoshimi Suzuki[a], Kenshi Kuma[c]
Ichiro Yasuda[d], Koji Suzuki[e], and Takeshi Nakatsuka[f, g]

[a]Institute of Geosciences, Shizuoka University, 836, Oya, Surugaku, Shizuoka 422-8529, Japan

[b]Research Institute of Green Science and Technology, Shizuoka University, 836, Oya, Surugaku, Shizuoka 422-8529, Japan

[c]Faculty of Fisheries Sciences, Graduate School of Fisheries Sciences, School of Fisheries Sciences, Hokkaido University, 3-1-1, Minato-cho, Hakodate, Hokkaido 041-8611, Japan

[d]Atmosphere and Ocean Research Institute, The University of Tokyo, 5-1-5, Kashiwanoha, Kashiwa-shi, Chiba 277-8564, Japan

[e]Faculty of Environmental Earth Science, Hokkaido University, Kita-10, Nishi-5, Kita-ku, Sapporo 060-0810, Hokkaido, Japan

[f]Pan-Okhotsk Research Center, Institute of Low Temperature Science, Hokkaido University, Kita-19, Nishi-8, Kita-ku, Sapporo 060-0819, Hokkaido, Japan

[g]Present address: The Research Institute for Humanity and Nature, 457-4 Motoyama, Kamigamo, Kita-ku, Kyoto 603-8047, Japan

[*]Corresponding author
Rumi Sohrin
Institute of Geosciences, Shizuoka University
Address: 836 Oya, Surugaku, Shizuoka 422-8529, Japan
E-mail: srsohri@ipc.shizuoka.ac.jp
Phone: +81-54-238-4934 Fax: +81-54-238-0491

Keywords: dissolved organic carbon (DOC); dissolved organic nitrogen (DON); transport; water mixing; Okhotsk Sea Mode Water (OSMW); North Pacific Intermediate Water (NPIW); Okhotsk Sea; subarctic North Pacific

Abstract

The Okhotsk Sea is considered the only ventilation source area for North Pacific Intermediate Water (NPIW), which is widely distributed in the low and middle latitudes of the North Pacific. Previous studies have confirmed high levels of dissolved organic carbon (DOC) in NPIW, yet the amounts and the processes driving DOC export from the Okhotsk Sea are poorly understood. In this study, concentrations of DOC and dissolved organic nitrogen (DON) were measured in the western Okhotsk Sea during the summer of 2006, and additional DOC measurements were made during the late spring of 2010. Results indicate that DOC transport to the intermediate waters (26.7–27.0 σ_θ) occurs through two processes. The first process involves the spread of water discharged from the continental shelf (Dense Shelf Water), which contributes to a DOC and turbidity maxima in the 250–300 m layer of Okhotsk Sea Mode Water (OSMW) located off the eastern Sakhalin coast. The second process involves diapycnal mixing in the Kuril Basin and the Bussol' Strait, where DOC is transported to a depth greater than 800 m. The ratio of DOC:DON in OSMW was significantly higher in the Kuril Basin and Bussol' Strait than off of the Sakhalin coast, which suggests that the transport of terrigenous organic matter from the bottom occurs in the former regions. DOC and DON efflux from the Okhotsk Sea to the intermediate layer in the North Pacific water (26.7–27.0 σ_θ) were estimated to be 68–72 Tg C yr^{-1} and 5.4 Tg N yr^{-1}, respectively, for which the DOC transported by diapycnal mixing accounts for 37%. We conclude that diapycnal mixing in the Kuril Basin and Bussol' Strait regions could play a significant role in regulating the quality and quantity of DOC exported to the intermediate water in the North Pacific.

1. Introduction

The Okhotsk Sea is one of the most productive marginal seas due to favorable light conditions and high inputs of macronutrients and iron from the Amur River (Sorokin and Sorokin, 1999; Liu et al., 2009; Nagao et al., 2010). Along with high autochthonous production, the Okhotsk Sea receives a significant amount of dissolved and particulate organic carbon (DOC and POC) from the Amur River. Large amounts of organic matter accumulate on the Siberian Shelf because of the high primary productivity in this area (Saitoh et al., 1996). The matter is then re-suspended by strong tidal mixing (Kowalik and Polyakov, 1998) and transported to the intermediate depths of the northern and northeastern Sakhalin coast via discharge of the shelf water, which is referred to as Dense Shelf Water (DSW) (Kitani, 1973). Nakatsuka et al. (2002, 2004) determined the distributions of DOC and POC in the area of the western Okhotsk Sea north of 53ºN in June, 2000. They estimated the terrestrial DOC input from the Amur River at 2.5 Tg C yr^{-1} from the linear regression intercept of a negative relationship between DOC and salinity in the surface water. They found high DOC concentration and turbidity in the water on the slope of the northeastern Sakhalin coast, which appears related to the discharge of DSW from the shelf. They estimated the inputs of DOC and POC from the shelf to the intermediate layer of the Okhotsk Sea via the discharge of DSW at 13.6 Tg C yr^{-1} and 0.9 Tg C yr^{-1}, respectively. These inputs were much higher than sinking POC flux (0.2 – 0.5 Tg C yr^{-1}) from the surface to the intermediate layer in the same area. The discharged DSW is further transported to the south along the East Sakhalin Current with mixing to the inflowing North Pacific Water. It eventually flows out to the North Pacific, mainly through the Bussol' Strait (Ohshima et al., 2002, 2010;

Katsumata and Yasuda, 2010), which is the largest and deepest (~2200 m) strait between the Kuril Islands.

The physical and biogeochemical studies in the Okhotsk Sea have led us to infer that the DOC exported from the Okhotsk Sea contributes substantially to biogeochemical cycling in the intermediate waters of the North Pacific. North Pacific Intermediate Water (NPIW) is comprised of the entire isopycnal layer (26.7–26.8 σ_θ), which is characterized by a salinity minimum found in the subtropical North Pacific gyre (Talley, 1997). Previous studies have suggested that large amounts of fresh (young) DOC enable NPIW to sustain higher prokaryotic productivity than the surrounding water masses (Nagata et al., 2001; Hansell et al., 2002), and the Okhotsk Sea is considered the main ventilation source area for NPIW (Itoh et al., 2003). However, the amount of and processes involved in DOC export from the Okhotsk Sea are not well understood due to a lack of DOC data from the southern Okhotsk Sea. This is particularly true for the Bussol' Strait, which is known as a site of water mass transformation driven by diapycnal mixing associated with strong tidal flow (Nakamura and Awaji, 2004; Nakamura et al., 2004; Ono et al., 2007). Furthermore, the fate of the DOC transported with the DSW has not been examined in the Sakhalin coast and the Kuril Basin (south end of the Okhotsk Sea). We hypothesize the following: (1) the DOC contained by the discharged DSW is transported to the Kuril Basin, which is then (2) exported down to greater depths in the Bussol' Strait by diapycnal mixing, (3) influencing the quality and quantity of the DOC exported to the intermediate water of the North Pacific. Because the ratio of DOC to dissolved organic nitrogen (DON) is indicative of the source and degradation state of dissolved organic matter (DOM), changes in the quality of DOM occurring with the mixing of water masses may be determined by comparing the DOC:DON ratios between the water masses (Anderson, 2002; Hopkinson et al., 2002). However, DON values from the Okhotsk Sea are not yet available. The purpose of this study is to evaluate the dynamics of DOM over the mixing processes in the Okhotsk Sea and to estimate their effluxes from the Okhotsk Sea to the intermediate North Pacific.

2. Materials and methods

2.1. Sampling

Seawater samples were taken in the western part of the Okhotsk Sea during the kh06 cruise of the R/V Professor Khromov (Far Eastern Regional Hydrometeorological Research Institute, Russia) conducted in the summer (August 13–September 14) of 2006. Vertical sampling was made at 36 stations using Niskin-X bottles mounted on a CTD-sampling system, and the surface seawater was collected at 25 northern stations by casting a plastic bottle with a spigot (Fig. 1). Sampling bottles were recovered and placed in a tent on the deck. Seawater for DOC and DON analyses was filtered with a pre-combusted Whatman GF/F filter (diameter, 47 mm) by connecting a spigot of the sampling bottle with silicone tubing to an inline plastic filter holder. Filtrates were collected in pre-combusted glass vials with Teflon-lined caps in duplicates and stored in a freezer until analysis. All materials were washed with detergent and 10% HCl before the cruise, and plastic gloves were worn during the processing of samples to avoid contamination. Additional vertical sampling was conducted at 9 stations in the late spring (May 25–June 7) of 2010 during the kh10 cruise of the R/V Professor Khromov to examine temporal changes in DOC distribution.

2.2. Analyses of DOC and DON

2.2.1. Instrument settings

Concentrations of DOC and total dissolved nitrogen (TDN) in the kh06 samples were simultaneously measured using a TOC-V total carbon analyzer equipped with a TNM-1 chemiluminescence detector unit (Shimadzu, Japan). We modified the catalyst packing of a combustion column of TOC-V and increased the flow rate of the compressed air introduced to an O_3 generator of TNM-1 from 0.5 to 0.8 L min^{-1} to improve the conversion efficiency of nitrogen (N) compounds to an excited NO_2 state. Details of this modification are shown in Figure S1. These modifications gave reliable DOC and DON measurements for the reference seawater (see 2.2.3), but actual conversion efficiency was not evaluated with regards to N-containing compounds such as amino acids. To save maintenance and running time, DOC concentration in the kh10 samples was measured using a TOC-5000A total carbon analyzer (Shimadzu) according to Sohrin and Sempéré (2005).

2.2.2. Routine analysis

During routine analysis, samples were thawed at room temperature, well mixed, and acidified with 2N HCl (1.0% vol/vol). Samples were then high-purity air bubbled through at a flow rate of 150 mL min^{-1} for 1.5 min within the syringe of TOC-V or at 50 mL min^{-1} for 10 min within a vial for the analysis on TOC-5000A. An injection of 100 μL of the bubbled sample was introduced to the combustion column, with the analysis generally repeated 3–5 times. To obtain a procedural blank, Milli-Q water was analyzed every four samples, and the average of the pooled peak areas of the Milli-Q water analyses collected over the entire analysis day was then subtracted from the seawater samples' peak area. NO_3^- accounted for >99% of the dissolved inorganic nitrogen (DIN, $[DIN] = [NO_3^-] + [NO_2^-] + [NH_4^+]$) in most (95%) of the samples collected from the intermediate water of the Okhotsk Sea and is expected to be most abundant N-compound in these samples. Therefore, we chose NO_3^- as a calibration standard compound of TDN analysis to minimize the analytical errors associated with differences in conversion efficiency among N-compounds. A calibration curve was obtained by the analysis of four distinctive concentrations of standard solution. This was prepared every analysis day by dilution of stock solutions of potassium hydrogen phthalate and potassium nitrate with freshly supplied Milli-Q water. Only potassium hydrogen phthalate was included for the analysis with TOC-5000A. The vertical series of samples were all analyzed on the same day.

After the DOC and TDN analyses, the remaining sample waters were kept in the dark at 0 °C for DIN analysis. Measurements of DIN were performed in duplicated aliquots using TRAACS 2000 (Bran+Luebbe) according to Hansen and Koroleff (1999) on the same day or the next day of the DOC and TDN analyses. Concentrations of DON were obtained by subtracting the average DIN concentration from the average TDN concentration.

2.2.3. Precisions and accuracy

The precision of triplicate or quadruplicate analyses were found to have average coefficients of variation (CV) of 1.5% (DOC) and 2.8% (TDN) on TOC-V and TMN-1, and 1.9% (DOC) on TOC-5000A. Precisions of DON concentrations and DOC:DON ratios were both 12% in average CV and were calculated using the precisions of DOC and TDN. The lower precision of DON and DOC:DON was attributed to the low DON concentration.

DOC and TDN concentrations in the reference seawater (DSR; distributed by D. Hansell Laboratory, University of Miami) were measured every routine analysis day to check the accuracy and consistency of our analysis. Low carbon water (LCW) from Hansell Laboratory was also measured to check the carbon and nitrogen contents in Milli-Q water supplied in our lab. There was no significant difference in DOC measurements between LCW and Milli-Q water over the analyses (average ± standard deviation of the difference, -0.3 ± 1.3 μmol C L^{-1}, n = 41; Student's t-test, p > 0.05), and the peak area of TDN analyses was always 0 both for LCW and Milli-Q water. The average peak area of the LCW analysis was subtracted from the DSR measurements to obtain DOC and TDN concentrations in DSR. DOC and TDN concentrations in DSR were 41.8 ± 1.1 μmol C L^{-1} and 33.1 ± 0.7 μmol N L^{-1}, respectively (n = 37) over the analyses of the kh06 samples, and 43.4 ± 0.9 μmol C L^{-1} (n = 8) over the DOC analyses of the kh10 samples. Although the DOC measurements were significantly higher for the analysis of the kh10 samples, the difference was quite small (~1.5 μmol C L^{-1}) and the values were well matched with their published values (DOC, 41–44 μmol C L^{-1}; TDN, 32.25–33.75 μmol N L^{-1}; http://www.rsmas.miami.edu/groups/biogeochem/CRM.html). We did not correct the possible systematic differences in the DOC measurements between the cruises.

Data for DON were unattainable for 30 of 430 samples due to machinery issues, such as failure in data storage, occurring during the TDN and DIN analyses. As high TDN measurements were obtained for DSR (34.8 μmol N L^{-1}), TDN values were corrected for the samples collected from Stn. A1 in the North Pacific by multiplying the TDN measurements by the ratio derived from the published TDN value of DSR (33.0 μmol N L^{-1})/TDN measurement of DSR (34.8 μmol N L^{-1}).

2.3. Analyses of salinity, turbidity, and chlorophyll *a*

Salinity was measured using an Autosal Salinometer. Turbidity (% transmission) was measured using a laser forescattering type of turbidity meter (Alec Electronics, ATU6-8M) mounted on a CTD-sampling system. Chlorophyll *a* (Chl *a*) concentration was measured according to the non-acidifying protocol of Welschmeyer (1994) after suspended particles were collected on GF/F filters and extracted Chl *a* in N, N-dimethylformamide at -20^{o}C (Suzuki and Ishimaru, 1990).

2.4. Statistics and calculation

Following the successful verification of normality and equal variance by the Shapiro-Wilk test and Levene Median test, respectively, differences between the groups were then tested by the Student's *t*-test or ANOVA. In cases of non-normality, a Mann-Whitney U-test was applied to examine the differences between two groups. For calculation of the inventories of the intermediate waters (26.7–27.0 σ_θ), DOC and DON concentrations at the 26.7σ_θ and 27.0 σ_θ density levels were obtained by linear interpolation with regards to the stations where a 26.7–27.0 σ_θ density range was present. Regarding the stations where water depth was shallower than the depth of 27.0 σ_θ level, inventory was calculated between the 26.7σ_θ level and the deepest sampling depth.

3. Results and Discussion

3.1. Distributions of DOC and DON in the surface water

Distinctively low salinity and high DOC and DON concentrations were found from depths of 0–5 m at the stations closest to the Amur River mouth (Stns. G8 and G10) during the kh06 cruise, indicating a DOC and DON supply originating from the Amur River (Fig. S2). To examine the influence of riverine discharge on DOC and DON distributions in the study area, DOC and DON concentrations in the surface water (0–5 m) were plotted as a function of salinity or Chl *a* (Fig. 2). High DOC recorded from a depth of 0 m at Stn.G14 (299 μmol C L^{-1}, Fig. S2) was considered an error and omitted from Figure 2 due to suspected contamination by volatile organic carbon during storage. Surface DOC and DON concentrations were negatively correlated to salinity and positively correlated to Chl *a* concentrations (Fig. 2). Changes in salinity explained 99% and 90% of the surface variations for DOC and DON, respectively, whereas variations in Chl *a* explained 44% (DOC) and 72% (DON) of the variation. These results indicate the strong influence of water from the Amur River on the distribution of surface DOC and DON across the study area. This is likely a consequence of high fluvial DOC concentrations found at the mouth of the Amur River (500−830 μmol C L^{-1}; Nagao et al., 2008, Levshina and Karetnikova, 2008). The linear regression equation between the surface DOC and salinity was expressed as $[DOC] = -(21.3 \pm 0.3) \times \text{salinity} + (756 \pm 10)$ ($r = -0.99$, $n = 68$; Fig. 2). A similar relationship ($[DOC] = -18.7 \times \text{salinity} + 691$) was reported by Nakatsuka et al. (2004) at a sampling location north of 53°N of our study area, between the 0–5 m layer, in June, 2000.

The molar ratio of the surface DOC:DON significantly decreased from 37.1 to 12.1 with increasing salinity from 16.69 to 33.39 ($r = -0.87$, $n = 57$) (Fig. 2). The negative correlation appears to reflect the mixing of fluvial DOM (high DOC:DON) with marine DOM (low DOC:DON) rather than any progress in the microbial degradation of DOM. This is due to the fact that the latter process generally raises DOC:DON ratios regardless of the origin of DOM (*i.e*. fluvial versus marine; Wiegner and Seitzinger, 2001; Hopkinson et al., 2002; Lønborg and Søndergaard, 2009). Previous studies have reported higher DOC:DON ratios in terrestrial waters adjacent to forest sites (20.5–103.1) compared to urban and agricultural sites (9.5–19) (Table S1). The observed high DOC:DON ratios (37.1) may reflect the structure of the Amur River watershed, which is dominated by forest and forested wetland of mixed broadleaf and meadows of sedge-reed grass and forbs, with minor contributions from settlement and agricultural land (Yermoshin et al., 2007).

The surface water during kh10 (late spring of 2010) was distinctively characterized from that in kh06 (summer of 2006) by colder water temperature and higher Chl *a* concentrations (Fig. S3). From these results and the monthly satellite observations of the surface Chl *a* distribution (Courtesy of JAXA/TOKAI UNIVERSITY), the study area was considered to be in progress of blooming during kh10 and in a post-bloom condition during kh06. In spite of the different water situations, surface DOC concentrations were similar between the cruises (Figs. 2 and S3).

3.2. Distributions of DOC and DON in DSW

Dense Shelf Water (DSW; > 26.7 σ_θ, <-1°C) forms mostly (50–70%) on the Siberian Shelf between January and March when sea ice formation and brine rejection occur (Martin et al., 1998; Gladyshev et al. 2000; Shcherbina et al., 2003), and a substantial fraction (55%) of the DSW remains on the shelf until May and June (Gladyshev et al., 2000). Temperature in the DSW at Stn. MP2 during kh10 (-1.79 – -1.75 °C), which is the nearest station to the Siberian Shelf, was close to the freezing temperature of the surface seawater with the same salinity (-1.8 °C) (Table 1, Fig. 1). Because pure DSW is defined as water at the freezing temperature (Itoh et al., 2003), the DSW found at Stn. MP2 appears to be less mixed with the surrounding water. DSW was also observed on the shelves of the Sakhalin Bay and the eastern Sakhalin coast (Table 1), where DSW is considered to have been transported from the Siberian Shelf (Gladyshev et al., 2000). There was no significant difference in DOC concentrations in DSW among the shelves (ANOVA, $F = 0.763$, $p > 0.1$), and the average (60.0 ± 4.6 μmol C L^{-1}, ± standard deviation) was close to the concentrations found in the DSW in the Sakhalin Bay and near the northeastern Sakhalin coast in June, 2000 by Nakatsuka et al. (2004) (61–75 μmol C L^{-1}). Similarly to the finding of Nakatsuka et al. (2004), DOC concentration and turbidity increased concomitantly near the bottom, where turbidity was indicated by the decrease in %transmission (Table 1). This result suggests the re-suspension of accumulated organic matter from the continental shelf during the formation and discharge of DSW (Nakatsuka et al., 2002, 2004). Yoshikawa et al. (2006) reported a very low N* value of -11 for the DSW on the Siberian Shelf, which is indicative of the progress of denitrification. They demonstrated that a low N* value is not caused by denitirification in the DSW but by sedimentary denitrification. N* values ranged between -17.6 and -10.1 in kh06, indicating a supply of dissolved compounds from the sediment to the DSW. DOC:DON ratios in the DSW varied among the stations, with lower ratios at the northern stations (11–15, Stns. G2 and F7) and an overall average of 18 ± 5 ($n = 17$). These DOC:DON ratios are lower than the DOC:DON ratios

(> 37.1) of fluvial organic matter inferred from Figure 2, and a substantial contribution of autochthonous DOM is suggested for the DSW. It should be noted that signatures of terrestrial plant materials were detected in the surface sediment on the Siberian Shelf (Seki et al., 2006), which implies that DSW may contain terrestrial organic carbon when it disturbs the sediment surface during discharge from the shelf.

3.3. Distributions of DOC and DON in Okhotsk Sea Mode Water (OSMW)

3.3.1. Off the Sakhalin coast

DSW is transported southward along the East Sakhalin Current and contributes to the Okhotsk Sea Mode Water (OSMW; 26.7–27.0 σ_θ, $\theta \geq 0$ °C) found off the eastern Sakhalin coast (Yasuda, 1997; Gladyshev et al., 2003). OSMW is identified as a water mass with a low potential vorticity at approximately 26.8 σ_θ level. It is a mixture of DSW, inflowing North Pacific Water, and Soya Warm Current Water (Itoh et al., 2003). The potential temperature in OSMW increases eastward from the eastern Sakhalin coast due to the increasing contribution of warm North Pacific Water to OSMW (Gladyshev et al., 2003). Nakatsuka et al. (2004) reported a decrease in DOC concentration with increasing temperature in the intermediate water (26.7–27.0 σ_θ level) off the northeastern Sakhalin coast. OSMW was situated between depths of 74 and 792 m during kh06 and kh10, and concentrations of DOC and DON in the intermediate water were found to decrease with increasing temperature (data not shown). This result implies greater dilution of DOC and DON occurs with increased mixing due to the inflowing North Pacific Water.

Coincident occurrence of DOC and turbidity maxima was observed at approximately 26.8 σ_θ level (250–300 m) in the OSMW off the Sakhalin coast (e.g., Stns F1 and B1 in kh06), and DOC concentrations were 4–6 μmol C L^{-1} greater than the surrounding depths at the maxima (Fig. 3). At the same density level, minimum N* peak also occurred (data not shown), and these results imply an inflow of DSW into the OSMW. The occurrence of DOC and turbidity maxima and N* minima indicates that dissolved matter (DOC and inorganic nutrients) and suspended particles were not diffused but were retained in the OSMW in spite of the water mixing process. This is likely due to the vertical stability maxima located at the upper and lower boundaries of the OSMW (Gladyshev et al., 2000). To examine an effect of lateral DOC export from the Sakhalin shelf on the offshore DOC maxima, DOC distribution is plotted along east-west transects made during kh06 (Fig. 4). DOC concentration in the maxima was higher at the most offshore stations than at the nearest stations along Lines B (49.5°N) and D (54°N), suggesting that these offshore DOC maxima are associated with the DSW discharged from the Siberian Shelf rather than from the Sakhalin shelf.

DOC:DON ratios in the OSMW located off the Sakhalin coast (average, 17) were within the ratios of oceanic DOM (Bronk, 2002), suggesting the dominance of autochthonous marine DOM in OSMW. This view is consistent with the enriched $\delta^{13}C$ value of POC in the OSMW located off the northeastern Sakhalin coast (Nakatsuka et al., 2004). DON maxima were negligibly detected at most stations with the exception of Stn. B1 at depths where DOC maxima occurred (Fig. 3). A likely explanation is the low precision of the DON analysis, when assuming the DOC:DON ratio at the DOC maxima represents the average DOC:DON ratio for the OSMW located off the Sakhalin coast (17). In this case, values of 4–6 μmol C L^{-1} of excess DOC forming the maxima would be equivalent to <0.4 μmol N L^{-1} of excess DON from the surrounding depths, which is lower than the analytical precision of DON in the intermediate water (0.5 μmol N L^{-1}).

3.3.2. Kuril Basin and Bussol' Strait

DOC maxima were not obvious in or near the Kuril Basin (Stn. A6 in kh06 and Stn. A4 in kh06 and kh10) or at some stations in the Bussol' Strait (Stns. Bussol-9 and Urup-E in kh06 and Stn. BW1 in kh10) (Fig. 3). The lower boundary of OSMW (27.0 σ_θ) was located deeper in the Kuril Basin and Bussol' Strait (Fig. 3), suggesting the dispersion of DOC within the expanded OSMW. In fact, the downward replacement of the 26.8 σ_θ level was observed at a shallow site in the Bussol' Strait during kh06 (Itoh et al., 2010). The hypothesis attributing the downward transport of DOC in the Kuril Basin and the Bussol' Strait was investigated by plotting cross-sections of the lines connecting the stations located furthest offshore (Fig. 5). An isoline of 27.0 σ_θ increased in depth between the location in the Kuril Basin (Stn. A4) and the Bussol' Strait (Stns. Bussol-9 and BW1), reaching a maximum depth of ca. 600 m (kh10) or 800 m (kh06) in the Kuril Basin. An area of high DOC concentrations (≥47 μmol C L^{-1}) presumably follows the isoline of 27.0 σ_θ, penetrating down to 500–800 m in the Kuril Basin and the Bussol' Strait. This depth is greater than the extent of DOC transported via the formation of OSMW by isopycnal mixing of the DSW with the inflowing waters, which had been inferred from DOC maxima recorded off the eastern Sakhalin coast (<300 m; Fig. 3). Surface DOC concentrations were lower in the Bussol' Strait than off the eastern Sakhalin coast, which is presumably related to the low primary productivity and dilution with upwelling deeper water inferred from low Chl *a* concentrations and temperature in this region, respectively (Fig. S3).

Near the eastern slope of the Bussol' Strait (Stn. Bussol-13) during kh06, the DOC maximum was observed at 400 m (26.78 σ_θ). Here, turbidity was also found to be relatively higher than OSMW measurements collected at the other stations (Fig. 3). This DOC maximum appears to be largely due to contributions of DOC exported from the lower layer rather than DOC from the upper layer, as the DOC:DON ratio in OSMW (19 ± 4) was comparable to the ratio calculated for the lower layer (20) but was significantly higher than the DOC:DON ratio in the upper layer (15 ± 4) at Stn. Bussol-13 (Student's *t*-test, $p < 0.05$) (data not shown). Indeed, DOC:DON ratios in OSMW were significantly higher in the Kuril Basin and the Bussol' Strait (median, 19) than off the Sakhalin coast (median, 16) (Mann-Whitney U-test, $p < 0.01$), although the ratios were comparable between these two regions with regard to the upper and lower layers (Mann-Whitney U-test, $p > 0.1$) (Fig. 6). These results suggest that diapycnal mixing did not disturb the sediment surface in the sampling period, but it influenced the DOM composition of OSMW when it occurred near the bottom the last time. We infer that vertical mixing temporally occurring close to the bottom of the Bussol' Strait, as shown in a numerical experiment (Nakamura and Awaji, 2004), facilitates the temporal release of organic matter from the disturbed sediment. This occurs via the re-suspension and flushing out of DOM-rich pore-water and then transports DOC to the 26.8 σ_θ level by production of low potential vorticity water at around this level (Ono et al., 2007). This process can increase DOC:DON ratios in OSMW, if the terrigenous organic matter was accumulated on the bottom. Seki et al. (2006) detected signatures of terrestrial plant materials from the surface sediment and the sediment traps deployed at depths equal to or below the OSMW near the Kuril Basin. Higher contributions of lignin-related materials found in both the DOC and POC fractions in the lower NPIW (750 m), when compared to other depths in the subtropical North Pacific (Hernes and Benner, 2002), might be associated with the mixing processes occurring in the Bussol' Strait, with subsequent export into the North Pacific. The DOC and turbidity values detected in the OSMW were relatively low at the other sampling sites in the Bussol' Strait (Fig. 3). Spatial differences in the vertical profiles of DOC are presumably related to regional and temporal differences in the strength of vertical mixing around the Kuril Islands, which depends on the local topography and direction of tidal current (Itoh et al., 2010).

3.4. DOC fluxes in the intermediate waters

We attempted to evaluate DOC and DON fluxes in the intermediate waters of the Okhotsk Sea and the North Pacific, with the results presented in Figure 7. DOC and DON fluxes related to the DSW discharge were obtained by multiplying the average of the DOC and DON concentrations in the DSW (Table 1) by the annual average volume rate of the DSW discharge. The annual average rate of the DSW discharge was obtained from the annual volume production of the DSW, assuming a discharge time of 1 year, because the DSW is considered to be replaced every winter (Gladyshev et al., 2000). Annual production of the DSW was calculated from its proportional relationship to the maximum sea ice volume (Nihashi et al., 2009). This relation was established for the Siberian Shelf, and we applied the relationship to the entire shelf region. The maximum sea ice volume was obtained from the averaged sea ice area observed in February–March of 2006 (Nakanowatari et al., 2010), or the area predicted for winter of 2010 (http://wwwod.lowtem.hokudai.ac.jp/~ohshima/social/2011/sie_prediction.html), assuming the ice thickness of 1 m (Nihashi et al., 2009). The annual average rate of DSW discharge was estimated at 0.42 and 0.65 Sv (1 Sv = 10^6 m^3 s^{-1}) in 2006 and 2010, respectively, and the values are similar to the estimates in previous studies (0.24–0.6 Sv; Gladyshev et al., 2003). The DOC flux related to the DSW discharge was estimated at 9.8 Tg C yr^{-1} (2006) and 14 Tg C yr^{-1} (2010), averaging 12 Tg C yr^{-1}, and the corresponding DON was 0.67 Tg N yr^{-1} (2006). Our estimated DOC flux was comparable to the estimate by Nakatsuka et al. (2004) (13.6 Tg C yr^{-1}). This was based on a previous estimate of the rate of the DSW discharge and the regression result between DOC and temperature in the intermediate water in the northeastern Sakhalin coast, with the assumed temperature of -1.5 ºC for the DSW flowing out from the shelf. The estimated DOC and DON fluxes may contain an error introduced by representing the concentration in the discharged DSW by the results obtained in June and September because the rate of DSW discharge decreases substantially after May (Gladyshev et al., 2003; Shcherbina et al., 2003). Satellite Chl *a* observations (Courtesy of JAXA/TOKAI UNIVERSITY) suggest that extensive primary production occurs on the Siberian Shelf in March, which corresponds with the period after the end of DSW formation (Gladyshev et al., 2000). Therefore, the DOM produced under a bloom condition is considered to be an unlikely contributor to the DSW, excepting the supply via dissolution of the settled particles.

DOC and DON fluxes into the North Pacific were calculated by multiplying the DOC and DON concentrations in the Bussol' Strait by the volume of the outflow transported. We referred to the volume transport values obtained at the 0.1 σ_θ interval from direct observation during one tidal cycle in September, 2001 by Katsumata et al. (2004). Regarding the 26.7–27.0 σ_θ level, the DOC efflux into the North Pacific was evaluated at 68 Tg C yr^{-1} (Stn. Bussol-9 in kh06), 72 Tg C yr^{-1} (Stn. Bussol-13 in kh06), and 69 Tg C yr^{-1} (Stn. BW1 in kh10), averaging 69 ± 2 Tg C yr^{-1}. Total DOC efflux is evaluated at 135 Tg C yr^{-1} with regards to the whole density level (26.0–27.4 σ_θ), where the positive volume flux was observed by Katsumata et al. (2004). The DON efflux on the 26.7–27.0 σ_θ level is 5.3 Tg N yr^{-1} (Stn. Bussol-9 in kh06) and 5.5 Tg N yr^{-1} (Stn. Bussol-13), averaging 5.4 Tg N yr^{-1}, while the total DON efflux is 11 Tg N yr^{-1} with regards to the 26.0–27.4 σ_θ level. These estimates may contain errors introduced by the large seasonal variations in the amount of volume transport associated with the outflow (Katsumata and Yasuda, 2010).

DOC and DON added to OSMW via diapycnal mixing in the Kuril Basin-Bussol' Strait region can be calculated from the difference in the DOC (DON) inventory of OSMW between the eastern Sakhalin coast and the Kuril Basin-Bussol' Strait region. DOC inventory was 180 ± 20 g C m^{-2} (n = 10, n is a number of stations where whole density level of OSMW existed) off the eastern Sakhalin during kh06 and kh10. By subtracting this value from the DOC inventory at the stations in the Bussol' Strait, the depth-weighted average concentration of the added DOC via diapycnal mixing was estimated at 15.4–21.8 μmol C L^{-1}. By multiplying the volume transport for the 26.7–27.0 σ_θ level (3.58 Sv; Kastumata et al., 2004), the DOC flux added to OSMW via diapycnal mixing in the Kuril Basin-Bussol' Strait region was estimated at 21–30 Tg C yr^{-1} (25 ± 4 Tg C yr^{-1}, n = 3; n is a number of stations at Bussol' Strait excluding Stn. Urup-E in kh06, where DOC was not measured at 27.0 σ_θ level). In the same manner, the corresponding DON flux was estimated at 1.4 Tg N yr^{-1}. From these calculations and the assumption of conservative transport of the DOC and DON added to OSMW, the DOC flux from off the eastern Sakhalin coast to the Kuril Basin-Bussol' Strait region would be 41–48 Tg C yr^{-1} (44 ± 3 Tg C yr^{-1}), and the DOC flux added to OSMW off the eastern Sakhalin coast was estimated at 32 Tg C yr^{-1} (32–33 Tg C yr^{-1}) from the difference in DOC fluxes toward and away from the region. The corresponding DON fluxes are 4.0 Tg N yr^{-1} and 3.3 Tg N yr^{-1}, respectively.

We attempt to obtain a rough estimate of the residence time of OSMW from the DOC fluxes that were made with the assumption of conservative DOC transport. If our estimated residence time is comparable to the values in literature, the assumption of a conservative DOC transport would be verified. By using the volume of OSMW in the Okhotsk Sea (2.85×10^{14} m^3; Itoh et al., 2003) and the Kuril Basin (9.5×10^{13} m^3; Galdyshev et al., 2003), the depth-weighted average DOC concentrations off the Sakhalin and the Kuril Basin-Bussol' Strait region, and the DOC fluxes away from these regions, DOC pool size and residence time of OSMW were estimated at 117 Tg C and 2.7 yr (off the Sakhalin) and 58 Tg C and 0.9 yr (Kuril Basin-Bussol' Strait), respectively. These residence times are within a range of the estimates in previous studies; 1.4–7 years for the Okhotsk Sea (Wong et al., 1998; Itoh et al., 2003) and 290 days–~2 years for the Kuril Basin (Yasuda, 1997; Gladyshev et al., 2003; Ohshima et al., 2010). A sum of the residence time of the DSW (~1 year) and OSMW (3.6 year) reveals that DOC produced in the surface water of the shelf region would reach the intermediate North Pacific after ~5 years. Although a part of semi-labile DOC (assumed turnover of months to years; Hansell et al., 2012) might reach the North Pacific, its bioavailability remains uncertain. High prokaryotic productivity found in NPIW (Nagata et al., 2001) might be partly supported by the DOC added via diapycnal mixing in the Bussol' Strait. Previous studies have revealed that transport of the upper layer water down to below the

OSMW occurs in the Bussol' Strait by diapycnal mixing (Yamamoto-Kawai et al., 2004; Ono et al., 2007), which is consistent with the low surface water temperature in this region (Fig. S2). Because current near the surface is about 10-fold faster than OSMW with turnover time of 0.5 year (Ohshima et al., 2002), diapycnal mixing in the Bussol' Strait can transport two distinct, relatively fresh DOM pools into OSMW: laterally transported DOM from the northern surface water by the surface current and the autochthonous DOM produced in the surface water of the Bussol' Strait. These are possible carbon sources that support high prokaryotic productivity in NPIW.

As a result, production of OSMW off the eastern Sakhalin coast and in the Kuril Basin-Bussol' Strait region contributes more to the efflux of DOM into the North Pacific (DOC, 46% and 37%; DON, 61% and 27%, respectively) than does the discharge of DSW (DOC, 17%; DON, 12%) (Fig. 7). Our results suggest that production of OSMW via diapycal mixing in the Kuril Basin-Bussol' Strait region is an important process for DOM export in terms of quantity and quality.

3.5. North Pacific

In the North Pacific, DOC concentrations were measured near the Bussol' Strait (Stn. A1) during kh06 and kh10 and the Kruzenshtern Strait (Stn. BNK2) during kh10. The Kruzenshtern Strait is a passage through which the greatest amount of the North Pacific Water inflows to the Okhotsk Sea (Katsumata and Yasuda, 2010). DOC concentration largely differed in the intermediate water (26.7–27.0 σ_θ) between kh06 and kh10, with the highest concentration of 63.6 μmol C L^{-1} (Stn. A1 in kh06) and 50.3 μmol C L^{-1} (Stn. A1 in kh10) (Fig. 3). The highest DOC concentrations, found at 26.8 σ_θ, were comparable between Stns. A1 and Bussol-13 during kh06, suggesting that the intensive transport of water with high DOC concentrations occurs at 26.8 σ_θ, and previous studies have reported the strongest outflow occurring at around 26.8 σ_θ (Wong et al., 1998; Katsumata et al., 2004; Katsumata and Yasuda, 2010). By applying a water mass analysis of Ono et al. (2007), the 26.8–27.2 σ_θ level at Stn. A1was found within the values of the waters in the Kuril Basin and the East Kamchatka Current during kh06, while it was similar to the property of the water in the East Kamchatka Current (East Kamchatka Current Water) during kh10 (Fig. 8). This result suggests that the intermediate water at Stn. A1 was more influenced by the East Kamchatka Current Water at the sampling period during kh10. The East Kamchatka Current is a part of the cyclonic circulation of the Western Subarctic Gyre and flows southward from the Bering Sea. A strong flow (8 Sv) is estimated at the 26.7–27.0 σ_θ level of the East Kamchatka Current Water near Stn. A1 (Iwao et al., 2003), which is equal to or larger than a volume transport of the Okhotsk Sea outflow through the Bussol' Strait [4.3–8.8 Sv; Nakamura and Awaji (2004) and references therein]. The East Kamchatka Current Water and the outflowing Okhotsk Sea water produce the Upstream Oyashio water in the south of the southern Kuril Islands by isopycnal mixing, which is an important source of NPIW (Yasuda et al, 1997). The observed higher DOC concentration, associated with the outflowing Okhotsk Sea, suggests that the Okhotsk Sea is a more important source for DOC in NPIW than the Bering Sea. For a better understanding of DOM transport to NPIW, future studies may address the mixing of the outflowing Okhotsk Sea water and East Kamchatka Water in the vicinity of the Kuril Islands.

4. Conclusion

Distributions of DOC and DON in the western Okhotsk Sea were determined during the summer of 2006 and those of DOC during the late spring of 2010. The surface distributions of DOC and DON were strongly influenced by the Amur River water, with higher DOC and DON concentrations and DOC:DON ratios in lower salinity regions. Maxima of DOC and turbidity were coincident in the OSMW located off the eastern Sakhalin coast, suggesting a DOC transport associated with the discharged DSW presumably from the Siberian Shelf. DOC and turbidity maxima were not obvious and the thickness of OSMW increased in the Kuril Basin and the Bussol' Strait, where production of OSMW related to vigorous diapycnal mixing has been inferred in previous studies. DOC:DON ratios in OSMW were slightly high in the Kuril Basin and the Bussol' Strait, and may be related to the export of terrigenous organic carbon from bottom sediments via diapycnal mixing. Diapycnal mixing also appeared to transport fresh DOM from the surface to OSMW. Effluxes of DOC and DON to the intermediate North Pacific, which includes the NIPW density level, were 135 Tg C yr^{-1} and 11 Tg N yr^{-1}, respectively, on the 26.0–27.4 σ_θ density level [where a positive volume flux was observed by Katsumata et al. (2004)]; and 69 Tg C yr^{-1} and 5.4 Tg N yr^{-1} on the OSMW 26.7–27.0 σ_θ density level. Fluxes associated with the OSMW production were comprised by two processes: isopycnal mixing off the eastern Sakhalin coast, and diapycnal mixing in the Kuril Basin and the Bussol' Strait. Fluxes associated with the OSMW production contributed more to the effluxes into the intermediate North Pacific than the fluxes related to the DSW discharge, indicating the importance of water mass transformation in the open Okhotsk Sea for DOM export to NPIW.

Acknowledgments

We thank the captain, officers and crews on board the R/V Professor Khromov and all the participants in the kh06 and kh10 cruises. Special thanks are given to Dr. Yuri N. Volkov and the staffs of Far Eastern Regional Hydrometeorological Research Institute for their support and to Mr. H. Nakatsuji (Shizuoka Univ.) for DIN analysis. We are grateful to Dr. Jun Nishioka for cruise arrangement and the two anonymous reviewers for their valuable comments. This work was supported by the Amur-Okhotsk Project, promoted by the Research Institute for Humanity and Nature (RIHN), and by a grant from the Ministry of Education, Science, Sports and Culture, Japan (20221002).

References

Anderson, L. (2002) DOC in the Arctic Ocean. In D.A. Hansell, & C.A. Carlson, Biogeochemistry of marine dissolved organic matter (pp. 665-683). San Diego, CA: Academic Press.

Bronk, D.A. (2002) Dynamics of DON. In D.A. Hansell and C.A. Carlson, Biogeochemistry of Marine Dissolved Organic Matter (pp. 153-247). San Diego, CA: Academic Press.

Gladyshev, S., Martin, S., Riser, S., & Figurkin, A. (2000) Dense water production on the northern Okhotsk shelves: Comparison of ship-based spring-summer observations for 1996 and 1997 with satellite observations. Journal of Geophysical Research, 105, 26281-26229.

Gladyshev, S., Talley, L., Kantakov, G., Khen, G., & Wakatsuchi, M. (2003) Distribution, formation, and seasonal variability of Okhotsk Sea Mode Water. Journal of Geophysical Research, 108, 3186.

Hansell, D.A., Carlson, C.A., & Schlitzer, R. (2012) Net removal of major marine dissolved organic carbon fractions in the subsurface ocean. Global Biogeochemical Cycles, 26, GB1016.

Hansell, D.A., Carlson, C.A., & Suzuki, Y. (2002) Dissolved organic carbon export with North Pacific Intermediate Water formation. Global Biogeochemical Cycles, 16.

Hansen, H.P., & Koroleff, F. (1999). Determination of nutrients. In K. Grasshoff, K. Kremling, & M. Ehrhardt, Methods of Seawater Analysis (pp. 159-228). Weinheim: Wiley-VCH.

Hernes, P.J., & Benner, R. (2002) Transport and diagenesis of dissolved and particulate terrigenous organic matter in the North Pacific Ocean. Deep-Sea Research I, 49, 2119-2132.

Hopkinson, C., Vallino, J., & Nolin, A. (2002) Decomposition of dissolved organic matter from the continental margin. Deep-Sea Research II 49, 4461-4478.

Itoh, M., Ohshima, K.I., & Wakatsuchi, M. (2003) Distribution and formation of Okhotsk Sea Intermediate Water: An analysis of isopycnal climatological data. Journal of Geophysical Research, 108, 3258.

Itoh, S., Yasuda, I., Nakatsuka, T., Nishioka, J., & Volkov, Y.N. (2010) Fine- and microstructure observations in the Urup Strait, Kuril Islands, during August 2006. Journal of Geophysical Research, 115, C8004.

Iwao, T., Endoh, M., Shikama, N., & Nakano, T. (2003) Intermediate circulation in the northwestern North Pacific derived from subsurface floats. Journal of Oceanography, 59, 893-904.

Katsumata, K., Ohshima, K.I., Kono, T., Itoh, M., Yasuda, I., Volkov, Y.N., & Wakatsuchi, M. (2004) Water exchange and tidal currents through the Bussol' Strait revealed by direct current measurements. Journal of Geophysical Research, 109, C09S06.

Katsumata, K., & Yasuda, I. (2010) Estimates of non-tidal exchange transport between the Sea of Okhotsk and the North Pacific. Journal of Oceanography, 66, 489-504.

Kitani, K. (1973) An oceanographic study of the Okhotsk Sea: particularly in regard to cold waters. Bulltin / Far Seas Fisheries Research Laboratory, 9, 45-77.

Kowalik, Z., & Polyakov, I. (1998) Tides in the Sea of Okhotsk. Journal of Physical Oceanography, 28, 1389-1409.

Levshina, S.I., & Karetnikova, E.A. (2008). Species of organic substance geochemical migration and phytoplankton distribution in the system Amur River-Amur Liman. In T. Shiraiwa, Report on Amur-Okhotsk Project, Vol. 5 (pp. 47-51). Kyoto, Japan: Research Institute for Humanity and Nature.

Liu, H., Suzuki, K., Nishioka, J., Sohrin, R., & Nakatsuka, T. (2009) Phytoplankton growth and microzooplankton grazing in the Sea of Okhotsk during late summer of 2006. Deep-Sea Research I, 56, 561-570.

Lønborg, C., & Søndergaard, M. (2009) Microbial availability and degradation of dissolved organic carbon and nitrogen in two coastal areas. Estuarine, Coastal and Shelf Science, 81, 513-520.

Martin, S., Drucker, R., & Yamashita, K. (1998) The production of ice and dense shelf water in the Okhotsk Sea polynyas. Journal of Geophysical Research, 103, 27771-27782.

Nagao, S., Terashima, M., Seki, O., Takata, H., Kawahigashi, M., Kodama, H., Kim, V.I., Shesterkin, V.P., Levshina, S., & Makinov, A.N. (2010). Biogeochemical behavior of iron in the lower Amur River and Amur-Liman. In T. Shiraiwa, Report on Amur-Okhotsk Project, Vol. 6 (pp. 41-50). Kyoto, Japan: Research Institute for Humanity and Nature.

Nagao, S., Terashima, M., Tanaka, H., Seki, O., Kim, V.I., Shesterkin, V.P., Levshina, I.S., & Makhinov, A.N. (2008). Geochemical behavior of dissolved iron in waters from the Amur River, Amur-Liman and Sakhalin Bay. In T. Shiraiwa, Report on Amur-Okhotsk Project, Vol. 5 (pp. 21-25). Kyoto, Japan: Research Institute for Humanity and Nature.

Nagata, T., Fukuda, R., Fukuda, H., & Koike, I. (2001) Basin-scale geographic patterns of bacterioplankton biomass and production in the subarctic Pacific, July - September 1997. Journal of Oceanography, 57, 301-313.

Nakamura, T., & Awaji, T. (2004) Tidally induced diapycnal mixing in the Kuril Straits and its role in water transformation and transport: A three-dimensional nonhydrostatic model experiment. Journal of Geophysical Research, 109, C09S07.

Nakamura, T., Toyoda, T., Ishikawa, Y., & Awaji, T. (2004) Tidal Mixing in the Kuril Straits and Its Impact on Ventilation in the North Pacific Ocean. Journal of Oceanography, 60, 411-423.

Nakanowatari, T., Ohshima, K.I., & Nagai, S. (2010) What determines the maximum sea ice extent in the Sea of Okhotsk? Importance of ocean thermal condition from the Pacific. Journal of Geophysical Research, 115, C12031.

Nakatsuka, T., Toda, M., Kawamura, K., & Wakatsuchi, M. (2004) Dissolved and particulate organic carbon in the Sea of Okhotsk: Transport from continental shelf to ocean interior. Journal of Geophysical Research, 109, C09S14.

Nakatsuka, T., Yoshikawa, C., Toda, M., Kawamura, K., & Wakatsuchi, M. (2002) An extremely turbid intermediate water in the Sea of Okhotsk: Implication for the transport of particulate organic matter in a seasonally ice-bound sea. Journal of Geophysical Research, 29, 1757.

Nihashi, S., Ohshima, K.I., Tamura, T., Fukamachi, Y., & Saitoh, S. (2009) Thickness and production of sea ice in the Okhotsk Sea coastal polynyas from AMSR-E. Journal of Geophysical Research, 114, C10025.

Ohshima, K.I., Nakanowatari, T., Riser, S., & Wakatsuchi, M. (2010) Seasonal variation in the in-and outflow of the Okhotsk Sea with the North Pacific. Deep-Sea Research II, 57, 1247-1256.

Ohshima, K.I., Wakatsuchi, M., & Fukamachi, Y. (2002) Near-surface circulation and tidal currents of the Okhotsk Sea observed with satellite-tracked drifters. Journal of Geophysical Research, 107, 3195.

Ono, K., Ohshima, K.I., Kono, T., Itoh, M., Katsumata, K., Volkov, Y.N., & Wakatsuchi, M. (2007) Water mass exchange and diapycnal mixing at Bussol' Strait revealed by water mass properties. Journal of Oceanography, 63, 281-291.

Saitoh, S., Kishino, K., Kiyofuji, K., Taguchi, S., & Takahashi, M. (1996) Seasonal variability of phytoplankton pigment concentration in the Okhotsk Sea. Journal of Remote Sensing Society Japan, 16, 172-178.

Seki, O., Yoshikawa, C., Nakatsuka, T., Kawamura, K., & Wakatsuchi, M. (2006) Fluxes, source and transport of organic matter in the western Sea of Okhotsk: Stable carbon isotopic ratios of n-alkanes and total organic carbon. Deep-Sea Research I, 53, 253-270.

Shcherbina, A.Y., Talley, L.D., & Rudnick, D.L. (2003) Direct observations of North Pacific ventilation: brine rejection in the Okhotsk Sea. Science, 302, 1952-1955.

Sohrin, R., & Sempéré, R. (2005) Seasonal variation in total organic carbon in the Northeast Atlantic in 2000-2001. Journal of Geophysical Research, 110, C10S90, doi:10.1029/2004JC002731.

Sorokin, Y.I., & Sorokin, P.Y. (1999) Production in the Sea of Okhotsk. Journal of Plankton Research, 21, 201-230.

Suzuki, R., & Ishimaru, T. (1990) An improved method for the determination of phytoplankton chlorophyll using N, N-dimethylformamide. Journal of the Oceanographic Society of Japan, 46, 190-194.

Talley, L.D. (1997) North Pacific Intermediate Water transports in the mixed water region. Journal of Physical Oceanography, 27, 1795-1803.

Welschmeyer, N.A. (1994) Fluorometric analysis of chlorophyll a in the presence of chlorophyll b and pheopigments. Limnology and Oceanography, 39, 1985-1992.

Wiegner, T.N., & Seitzinger, S.P. (2001) Photochemical and microbial degradation of external dissolved organic matter inputs to rivers. Aquatic Microbial Ecology, 24, 27-40.

Wong, C.S., Matear, R.J., Freeland, H.J., Whitney, F.A., & Bychkov, A.S. (1998) WOCE line P1W in the Sea of Okhotsk 2. CFCs and the formation rate of intermediate water. Journal of Geophysical Research, 103, 15625-15642.

Yamamoto-Kawai, M., Watanabe, S., Tsunogai, S., & Wakatsuchi, M. (2004) Chlorofluorocarbons in the Sea of Okhotsk: Ventilation of the intermediate water. Journal of Geophysical Research, 109, C09S11.

Yasuda, I. (1997) The origin of the North Pacific Intermediate Water. Journal of Geophysical Research, 102, 893-909.

Yermoshin, V.V., Ganzey, S.S., Murzin, A.V., Mishina, N.V., & Kudryavtzeva, E.P. (2007). Creation of GIS for Amur River basin: the basic geographical information. In T. Shiraiwa, Annual Report on Amur-Okhotsk Project, Vol. 4 (pp. 151-159). Kyoto, Japan: Research Institute for Humanity and Nature.

Yoshikawa, C., Nakatsuka, T., & Wakatsuchi, M. (2006). Distribution of N* in the Sea of Okhotsk and its use as a biogeochemical tracer of the Okhotsk Sea Intermediate Water formation process. Journal of Marine Systems, 63, 49-62.

Figure captions

Figure 1. Schematic showing the study area where the kh06 (August–September, 2006; large circles) and kh10 (May–June, 2010; black circles) cruises were conducted. Measurements taken for the vertically collected samples are shown for each of the DOC collection stations.

Figure 2. Plots comparing salinity and chlorophyll *a* (Chl *a*) concentration with DOC and DON concentrations, and with DOC:DON ratios, for the surface waters measurements during the kh06 cruise and the corresponding relationships with DOC in the kh10 cruise. Lines were fitted by linear regression, with the regression results given in the plots.

Figure 3. Vertical profile plots showing concentrations of DOC and DON, and % transmission values measured in the upper 2000 m of the water column, at representative stations located in the distinctive regions. Station locations are shown in Fig. 1. Water depth is shown in parenthesis for values exceeding 2000 m. Shaded areas indicate the intermediate waters with densities of 26.7–27.0 σ_θ. Error bars indicate the standard deviation associated with the analyses. Note that smaller % transmission values correspond to higher turbidity levels.

Figure 4. Vertical section plots illustrating DOC concentrations along Lines B (49.5°N), C (52.25°N) and D (54°N) during the kh06 cruise. Locations are shown in Fig. 1. The broken lines indicate isopycnals of 26.7 σ_θ and 27.0 σ_θ. Dots are representative of the sampling depths of DOC.

Figure 5. Vertical section plots illustrating DOC concentrations along north-south transects during the kh06 (Line kh06) and kh10 (Line kh10) cruises. Locations are shown in Fig. 1. The broken lines indicate isopycnals of 26.7 σ_θ and 27.0 σ_θ. Dots are representative of the sampling depths of DOC.

Figure 6. Box plots of DOC:DON ratios in the distinctive layers off the Sakhalin coast and in the Kuril Basin-Bussol' Strait region. Upper (lower) ends of boxes and error bars show 75% (25%) and 90% (10%) confidence intervals (CI), and upper (lower) dots show 95% (5%) CI, respectively. Solid lines in boxes show medians. Asterisks denote the significantly different ratios between the regions. DOC:DON ratios in 0−5 m depths were excluded because of the influence of the Amur River water and the ratios at Stn. A6 were also excluded because of its location on the slope of the Kuril Basin. Number of data is shown in parenthesis. Note that 5%, 10%, 90% and 95% CI are not computed with regards to the samples with $n < 8$.

Figure 7. DOC and DON fluxes in the intermediate waters (26.7–27.0 σ_θ) of the western Okhotsk Sea and the North Pacific. Percentage values in parentheses represent the contributions of the fluxes to the efflux into the North Pacific. Periods in boxes are residence time of the intermediate waters that are assumed (Shelf) or calculated from the distribution of DOC (off Sakhalin and Kuril Basin-Bussol' Strait region). Note that total effluxes of DOC and DON to the intermediate North Pacific is 135 Tg C yr^{-1} and 11 Tg N yr^{-1}, respectively, with regards to the whole density level (26.0–27.4 σ_θ) where the positive volume flux was observed by Katsumata et al. (2004).

Figure 8. Comparison of potential temperature (θ)-salinity diagrams between the North Pacific (Stns. A1 and BNK2, circle) and the Kuril Basin (Stn. 4, triangle) during the kh06 (closed symbols) and kh10 (open symbols) cruises, with those of the East Kamchatka Current Water (solid line) and the OSMW in the Kuril Basin (Kuril Basin Water, broken line). The diagrams associated with the East Kamchatka Current Water and the Kuril Basin Waters are shown with potential temperature standard deviations at 0.1 σ_θ intervals, with reference to Ono et al. (2007).

Table 1

Table 1 . Physical and biogeochemical parameters and DOC and DON concentrations and their ratios in the DSW found in the shelf region.

Shelf (period)	Station	Water depth (m)	Depth (m)	θ (ºC)	Salinity	σ_θ	Transmission (%)	N* (μmol N L^{-1})	DOC (μmol C L^{-1})	DON (μmol N L^{-1})	DOC/DON (mol:mol)
Northwestern	MP2	140	49.6	-1.75	33.24	26.75	95.2	-[a]	55.7	-	-
(June, 2010)	(56.4ºN/140.2ºE)		98.7	-1.78	33.26	26.77	94.8	-	56.2	-	-
			123.7	-1.79	33.35	26.85	86.6	-	59.1	-	-
			129.1	-1.79	33.36	26.85	86.3	-	60.0	-	-
			134.6	-1.79	33.36	26.85	86.1	-	59.4	-	-
Sakhalin Bay	G2	135	73.5	-1.74	33.21	26.72	97.0	-11.5	55.0	5.1	10.7
(Sep, 2006)	(55.0ºN/141.0ºE)		100.1	-1.73	33.44	26.91	85.8	-15.6	59.7	4.5	13.4
			127.6	-1.71	33.45	26.92	68.3	-17.6	60.5	4.5	13.5
	G4	68	49.7	-1.26	33.25	26.75	92.6	-12.9	65.0	2.9	22.2
	(54.5ºN/141.0ºE)		62.5	-1.37	33.23	26.73	91.7	-16.2	66.8	3.2	20.9
	F7	200	148.9	-1.29	33.23	26.73	96.4	-10.1	54.7	3.9	14.0
	(55.5ºN/141.0ºE)		191.7	-1.47	33.44	26.90	78.0	-14.5	59.1	3.9	15.3
Eastern Sakhalin	E3	94	50.3	-1.18	33.29	26.78	93.3	-12.1	61.0	2.9	21.2
(Aug, 2006)	(54.5ºN/143.1ºE)		73.4	-1.31	33.30	26.78	93.2	-11.8	57.4	2.9	19.5
			88.0	-1.31	33.30	26.79	94.1	-11.9	55.8	2.6	21.2
	E1	99	74.7	-1.41	33.19	26.70	94.9	-11.3	62.3	2.6	23.7
	(54.4ºN/142.9ºE)		93.9	-1.45	33.20	26.71	95.0	-11.7	71.9	-	-
average ± standard deviation (n = 17)				-1.54±0.23	33.30 ± 0.09	26.79 ± 0.07	90.0 ± 7.5	-13.1 ± 2.3	60.0 ± 4.6	3.5 ± 0.9	17.8 ± 4.5

[a] -: not determined.

Figure 1

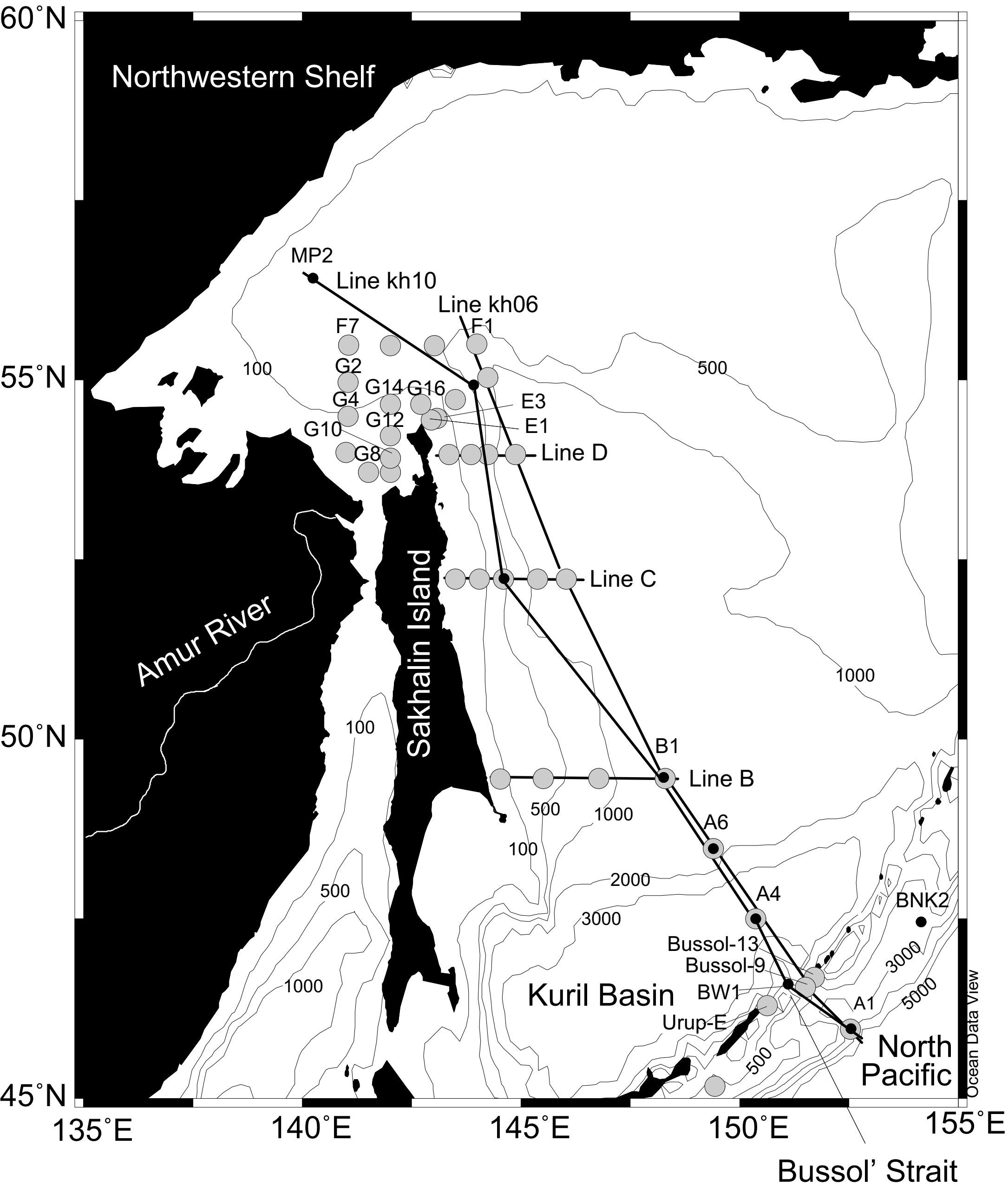

Fig. 1

Figure 2

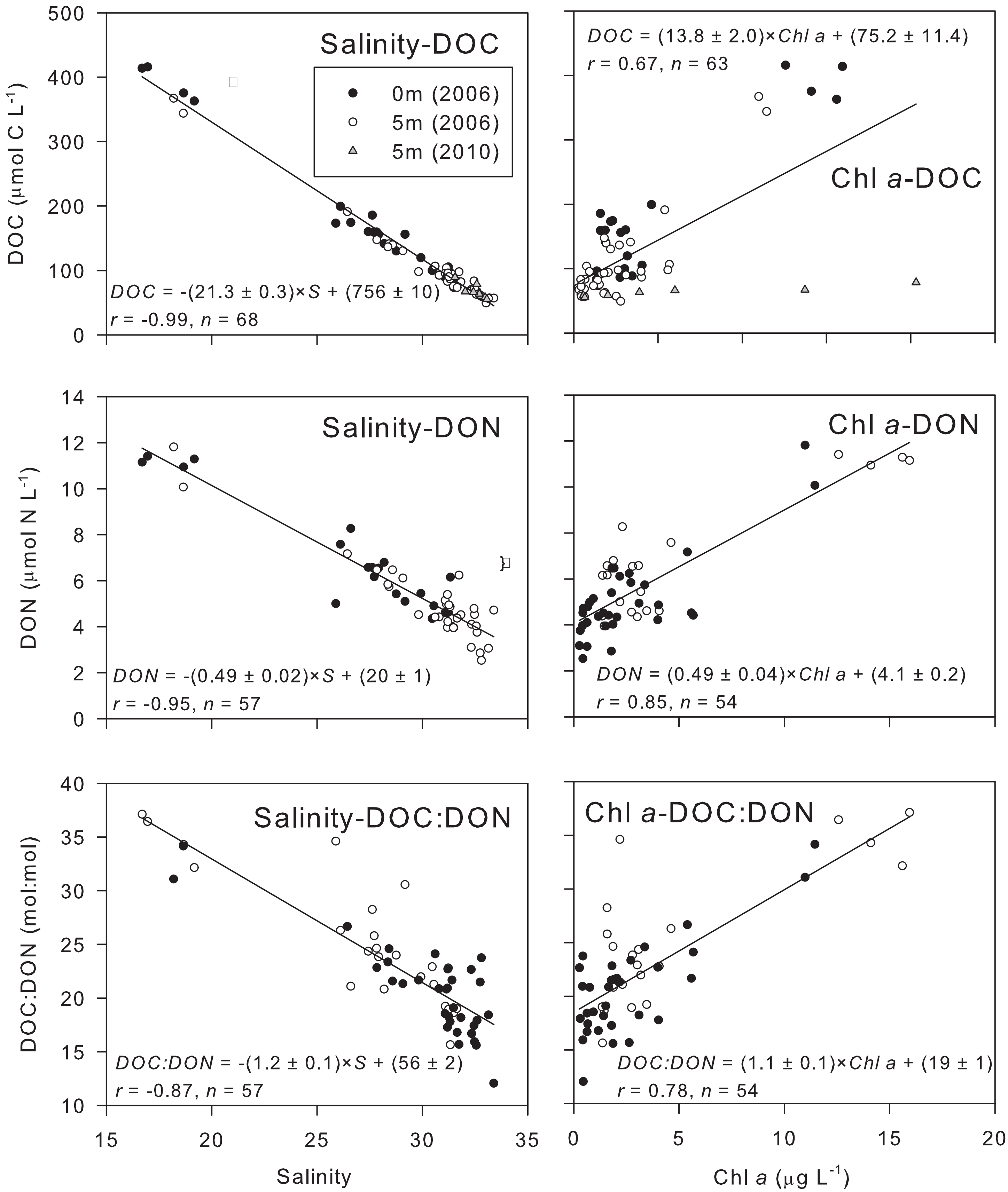

Salinity-DOC
0m (2006)
5m (2006)
5m (2010)
DOC = -(21.3 ± 0.3)×S + (756 ± 10)
r = -0.99, n = 68
DOC (μmol C L-1)
DOC = (13.8 ± 2.0)×Chl a + (75.2 ± 11.4)
r = 0.67, n = 63
Chl a-DOC
Salinity-DON
DON = -(0.49 ± 0.02)×S + (20 ± 1)
r = -0.95, n = 57
DON (μmol N L-1)
Chl a-DON
DON = (0.49 ± 0.04)×Chl a + (4.1 ± 0.2)
r = 0.85, n = 54
Salinity-DOC:DON
DOC:DON = -(1.2 ± 0.1)×S + (56 ± 2)
r = -0.87, n = 57
DOC:DON (mol:mol)
Chl a-DOC:DON
DOC:DON = (1.1 ± 0.1)×Chl a + (19 ± 1)
r = 0.78, n = 54
Salinity
Chl a (μg L-1)

Figure 3

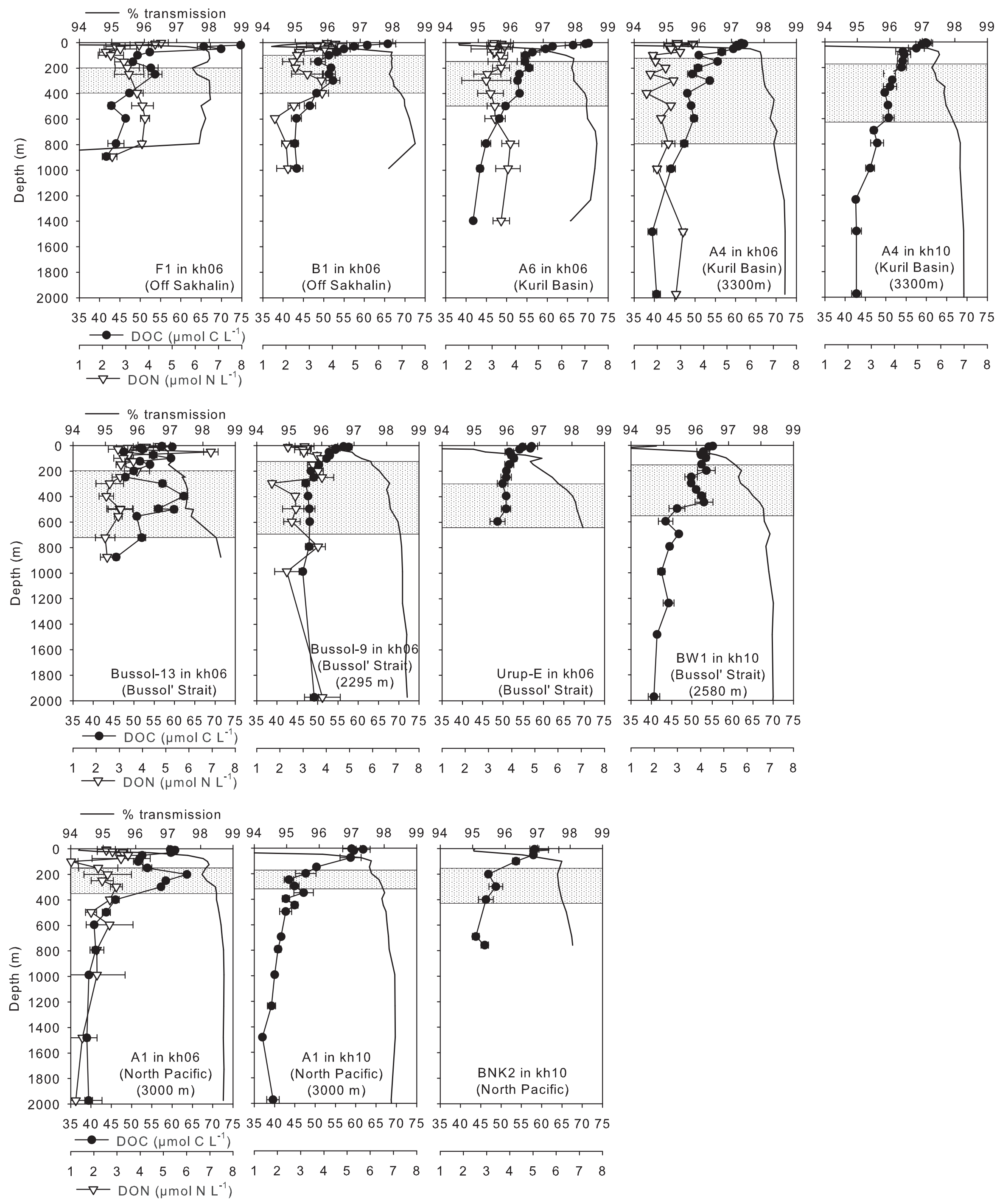
% transmission
Depth (m)
DOC (μmol C L-1)
DON (μmol N L-1)
F1 in kh06 (Off Sakhalin)
B1 in kh06 (Off Sakhalin)
A6 in kh06 (Kuril Basin)
A4 in kh06 (Kuril Basin) (3300m)
A4 in kh10 (Kuril Basin) (3300m)
Bussol-13 in kh06 (Bussol' Strait)
Bussol-9 in kh06 (Bussol' Strait) (2295 m)
Urup-E in kh06 (Bussol' Strait)
BW1 in kh10 (Bussol' Strait) (2580 m)
A1 in kh06 (North Pacific) (3000 m)
A1 in kh10 (North Pacific) (3000 m)
BNK2 in kh10 (North Pacific)

Figure 4

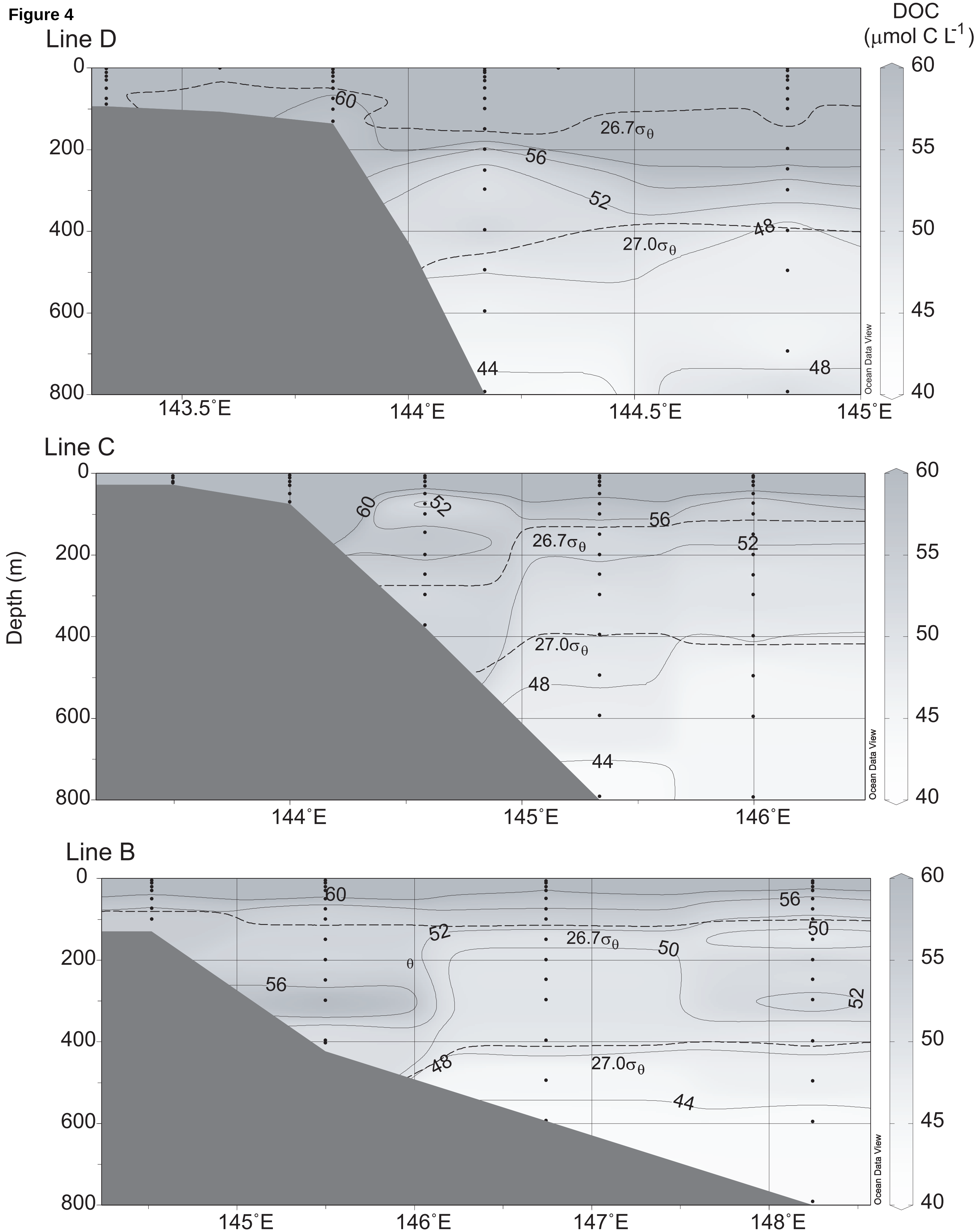

Fig. 8

Figure 5

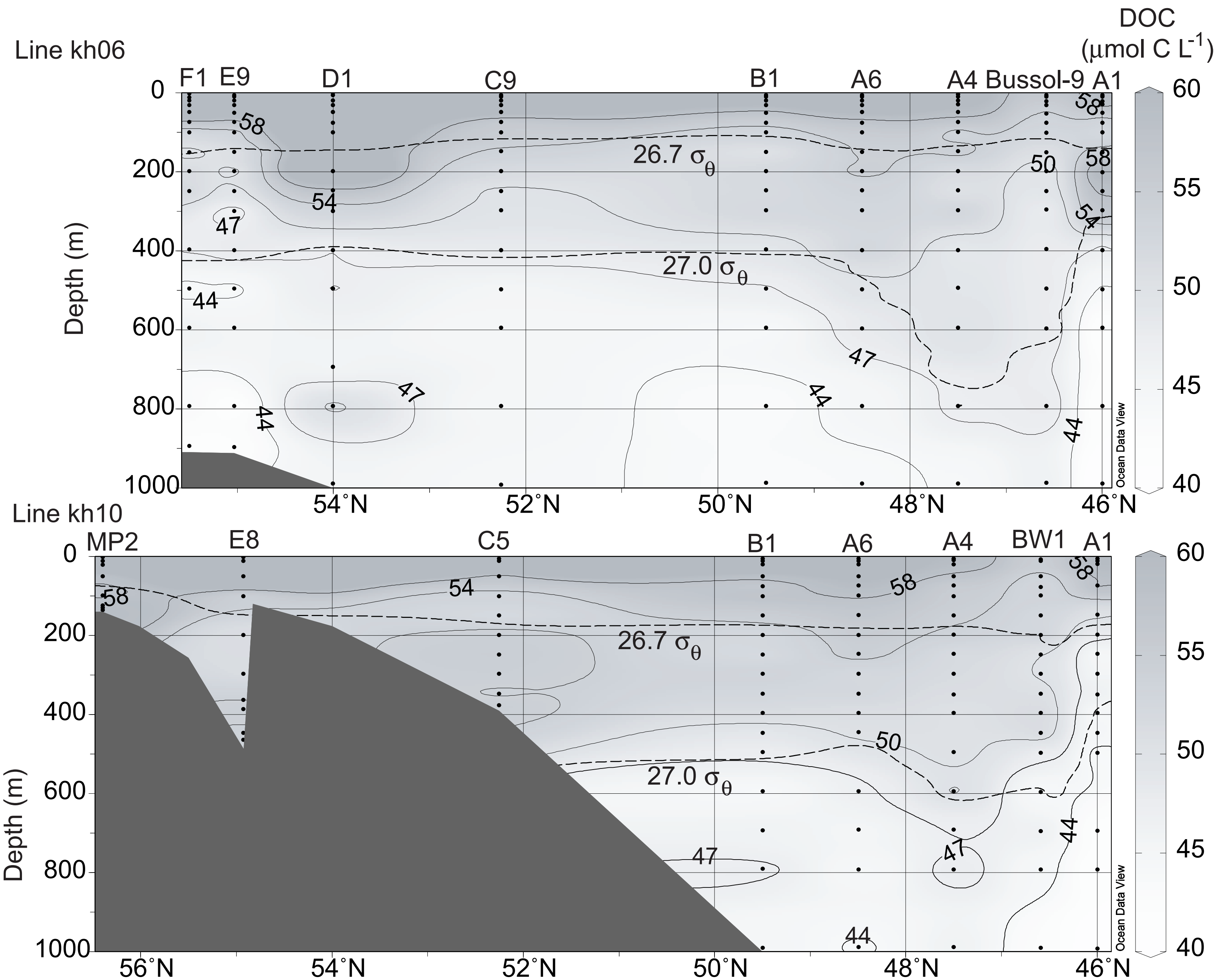

DOC
(μmol C L-1)
Line kh06
F1 E9 D1 C9 B1 A6 A4 Bussol-9 A1
Depth (m)
26.7 σθ
27.0 σθ
54°N 52°N 50°N 48°N 46°N
Line kh10
MP2 E8 C5 B1 A6 A4 BW1 A1
56°N 54°N 52°N 50°N 48°N 46°N
Ocean Data View

Figure 6

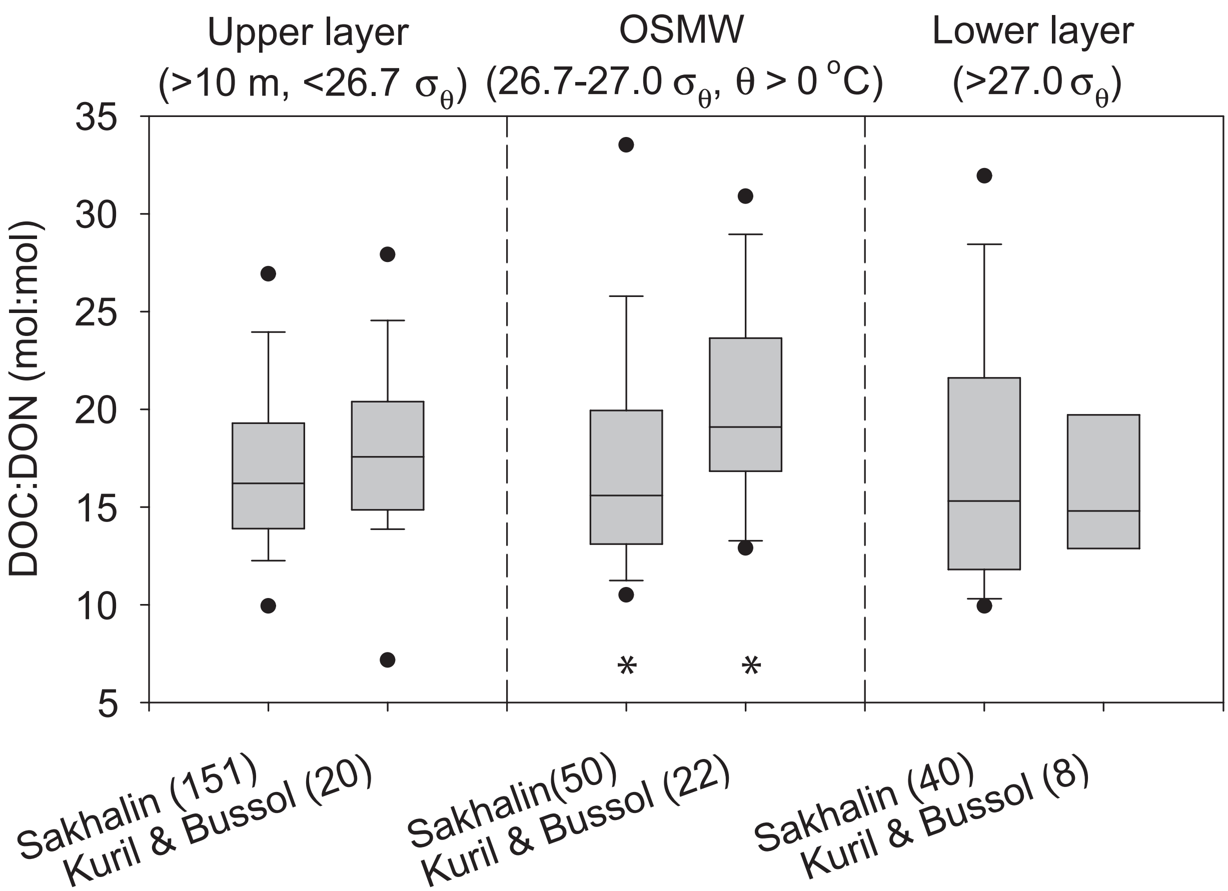

Fig. 10

Figure 7

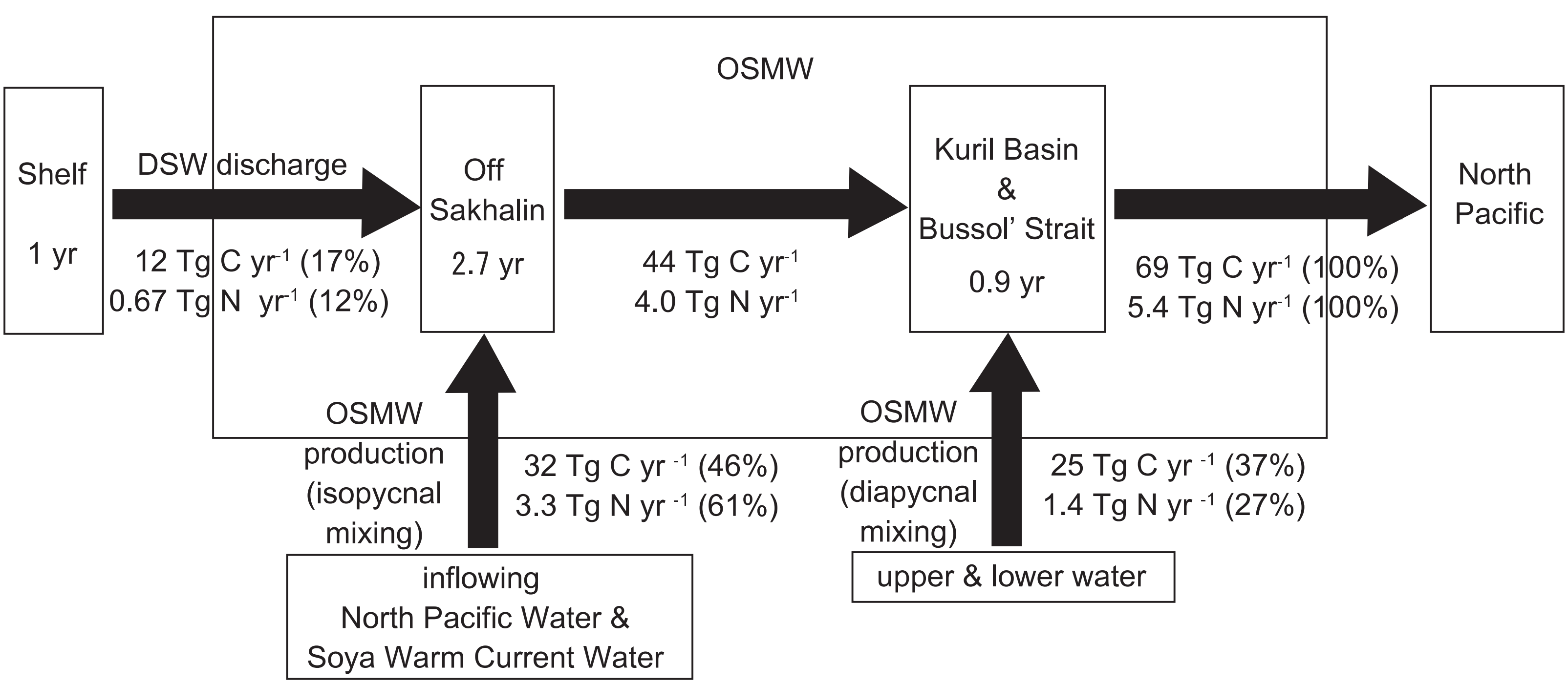
OSMW
Shelf
1 yr
DSW discharge
12 Tg C yr-1 (17%)
0.67 Tg N yr-1 (12%)
Off
Sakhalin
2.7 yr
44 Tg C yr-1
4.0 Tg N yr-1
Kuril Basin
&
Bussol' Strait
0.9 yr
69 Tg C yr-1 (100%)
5.4 Tg N yr-1 (100%)
North
Pacific
OSMW
production
(isopycnal
mixing)
32 Tg C yr -1 (46%)
3.3 Tg N yr -1 (61%)
inflowing
North Pacific Water &
Soya Warm Current Water
OSMW
production
(diapycnal
mixing)
25 Tg C yr -1 (37%)
1.4 Tg N yr -1 (27%)
upper & lower water

Figure 8

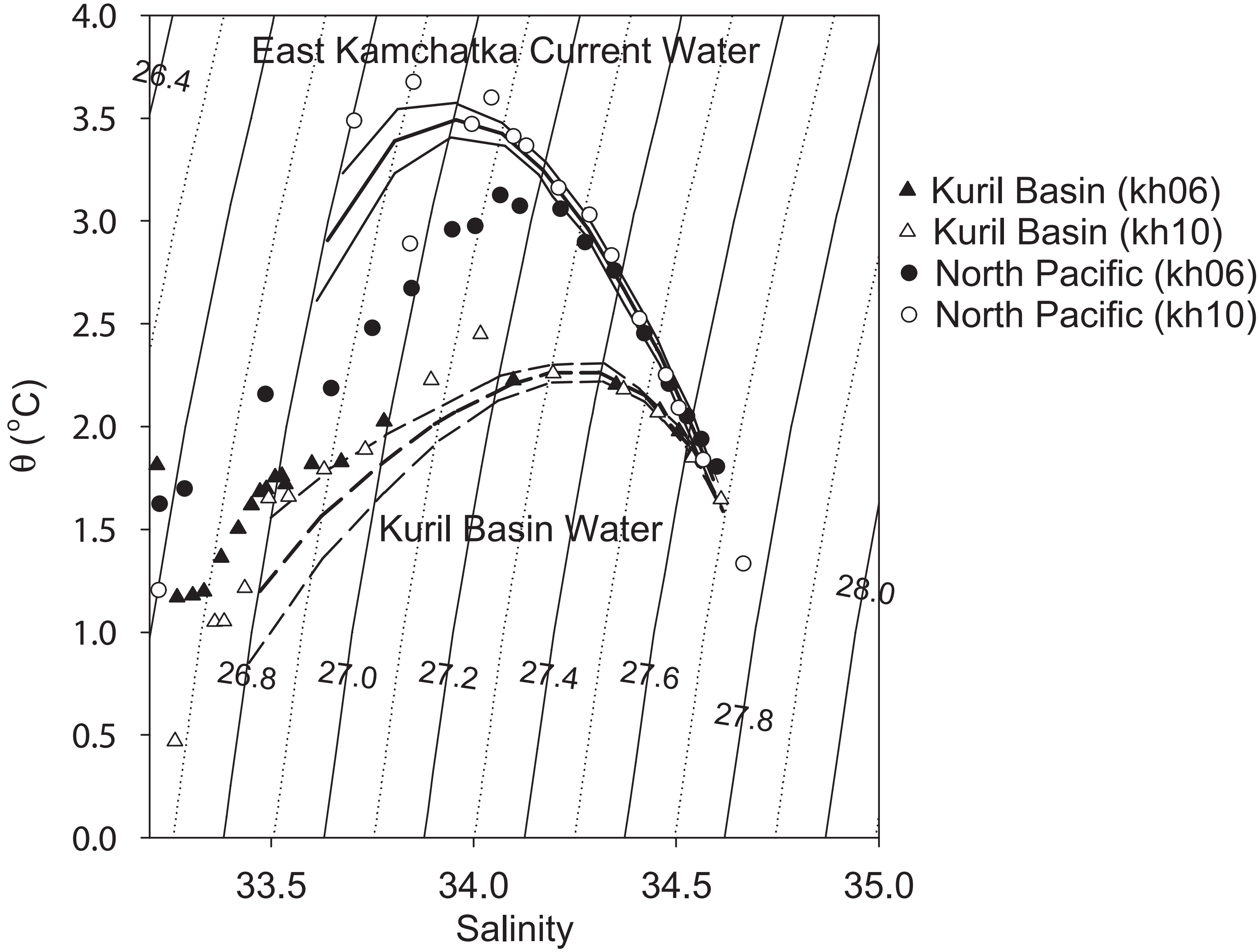

Fig. 12

Supplement (figure caption & Table S1)

Table S1. DOC/DON ratios in the surface fresh waters reported in previous studies.

Type and location	Catchment, watershed or sampling site[a]	DOC/DON	Reference
Riverine water at river mouth			
Tsengwen river	Suburban, rural and agricultural land	9.5	e
Atchafalaya River	wetland	16	f
Rhône River	Mountains, agricultural and urban lands[b]	19	g
River Tyne	Mostly open and afforested peatland	20.5-103.1	h
Mississippi River plume	Agricultural and urban lands[c]	30	f
Siberian rivers entering to the Arctic Ocean	Taiga and tundra	48.2 ± 13.6	i
		51 ± 9	j
Mackenzie River	Arctic tundra, boreal forest, peatland, and mountainous cordillera[d]	84.9	k
Soil solution			
New Jersey watersheds	Agricultural	10 ± 2	l
	Urban/suburban	18 ±1 2	
	Forest	53 ± 36	
Jeneau, Alaska	Fen	24.6 ± 2.6	m
	Upland forest	30.3 ± 3.4	
	Bog	34.1 ± 3.9	
	Forested wetland	49.7 ± 4.5	

[a] Sampling sites are shown for soil solution.

[b] Radakovitch,O., Roussiez, V., Ollivier, P., Ludwig, W., Grenz, C., Probst, J. -L. (2008), Input of particulate heavy metals from rivers and associated sedimentary deposits on the Gulf of Lion continental shelf. Estuarine, Coastal and Shelf Science, 77, 285-295.

[c] Donner, S. D. (2004) Impact of changing land use practices on nitrate export by the Mississippi River. Global Biogeochemical Cycles, 18, GB1028, doi:10.1029/2003GB002093.

[d] Dyke, L., and G.R. Brooks (2000) The physical environment of the Mackenzie Valley: A baseline for the assessment of environmental change. Geological Survey of Canada Bulletin 547.

[e] Hung, J.-J., & Huang, M.-H. (2005) Seasonal variations of organic-carbon and nutrient transport through a tropical estuary (Tsengwen) in southwestern Taiwan. Environmental Geochemistry and Health, 27, 75-95.

[f] Pakulski, J.D., Benner, R., Whitledge, T., Amon, R., Eadie, B., Cifuentes, L., Ammerman, J., & Stockwell, D. (2000) Microbial metabolism and nutrient cycling in the Mississippi and Atchafalaya River plumes. Estuarine, Coastal and Shelf Science, 50, 173-184.

[g] Pujo-Pay, M., Conan, P., Joux, F., Oriol, L., Naudin, J.J., & Cauwet, G. (2006) Impact of phytoplankton and bacterial production on nutrient and DOM uptake in the Rhône River plume (NW Mediterranean). Marine Ecology Progress Series, 315, 43-54.

[h] Spencer, R.G.M., Ahad, J.M.E., Baker, A., Cowie, G.L., Ganeshram, R., Upstill-Goddard, R.C., & Uher, G. (2007) The estuarine mixing behavior of peatland derived dissolved organic carbon and its relationship to chromophoric dissolved organic matter in two North Sea estuaries (U.K.). Estuarine, Coastal and Shelf Science, 74, 131-144.

[i] Lobbes, J.M., Fitznar, H.P., & Kattner, G. (2000) Biogeochemical characteristics of dissolved and particulate organic matter in Russian rivers entering the Arctic Ocean. Geochimica et Cosmochimica Acta, 64, 2973-2983.

[j] Dittmar, T., Fitznar, H.P., & Kattner, G. (2001) Origin and biogeochemical cycling of organic nitrogen in the eastern Arctic Ocean as evident from D- and L-amino acids. Geochimica et Cosmochimica Acta, 65, 4103-4114.

[k] Emmerton, C.A., Lesack, L.F.W., & Vincent, W.F. (2008) Nutrient and organic matter patterns across the Mackenzie River, estuary and shelf during the seasonal recession of sea-ice. Journal of Marine Systems, 74, 741-755.

[l] Seitzinger, S.P., Road, D., Sanders, R.W., & Styles, R. (2002) Bioavailability of DON from natural and anthropogenic sources to estuarine plankton. Limnology and Oceanography, 47, 353-366.

[m] Fellman, J.B., D'Amore, D.V., Hood, E., & Boone, R.D. (2008) Fluorescence characteristics and biodegradability of dissolved organic matter in forest and wetland soils from coastal temperate watersheds in southeast Alaska. Biogeochemistry, 88, 169-184.

Figure captions of supplementary material

Figure S1. Schematic of a catalyst packing in a combustion column located in a TOC-V analyzer used for DOC and TDN analyses. All materials were the original supplies for TOC-V, other than Cr_2O_3 (Elemental Microanalysis Ltd, UK), quartz wool (Tosoh SGM, Japan), and squared platinum mesh (Sumika Chemical Analysis Service Ltd, Japan). The grain size of Cr_2O_3 was selected according to Ogawa et al. (1999; Deep Sea Research I, 46, 1809-1826). It should be noted that the platinum ST-type catalyst (Shimadzu) placed on the top of the combustion column seems important for sustaining a sufficient oxidation efficiency of DOC, but is easily reduced to a powder form by repeated injections, resulting in decreasing measurement readings. To overcome this problem, the top ST catalyst was changed every 2–3 days of analysis. We also altered the flow rate of the compressed air introduced to an O_3 generator of TNM-1 from 0.5 to 0.8 L min^{-1}. Preliminary measurements of TDN in deep seawater (1000 m depth) from the Suruga Bay, central Japan, were conducted according to the manufacturer's protocol, but the measurement readings were lower (average, 36.2 μmol N L^{-1}) than the values obtained from colorimetric measurements of dissolved inorganic nitrogen (DIN, [DIN]= $[NO_3^-]$ + $[NO_2^-]$ + $[NH_4^+]$; 40.2 μmol N L^{-1}). The modification to the catalyst packing improved the TDN measurements for the Suruga Bay deep seawater to 40.1 μmol N L^{-1}, and the increase in airflow rate further improved the measurements to 42.9 μmol N L^{-1}. An increase in airflow rate alone was not found to improve the measurements (36.9 μmol N L^{-1}). We consider that these modifications have improved conversion efficiency of N-compounds sufficiently, since our TDN measurements for the reference seawater (Deep Seawater Reference, DSR; distributed by D. Hansell Laboratory, University of Miami) were comparable to its published value (see 2.2.3). However, analyses of standard N-compounds such as amino acids are necessary for more thorough evaluation of our improved method.

Figure S2. Vertical profile plots illustrating salinity and DOC and DON concentrations off the northern Sakhalin coast during kh06.

Figure S3. Bubble plots illustrating horizontal distributions of temperature (θ) and concentrations of Chl *a* and DOC obtained at 5 m depth during kh06 and kh10.

Fig S1

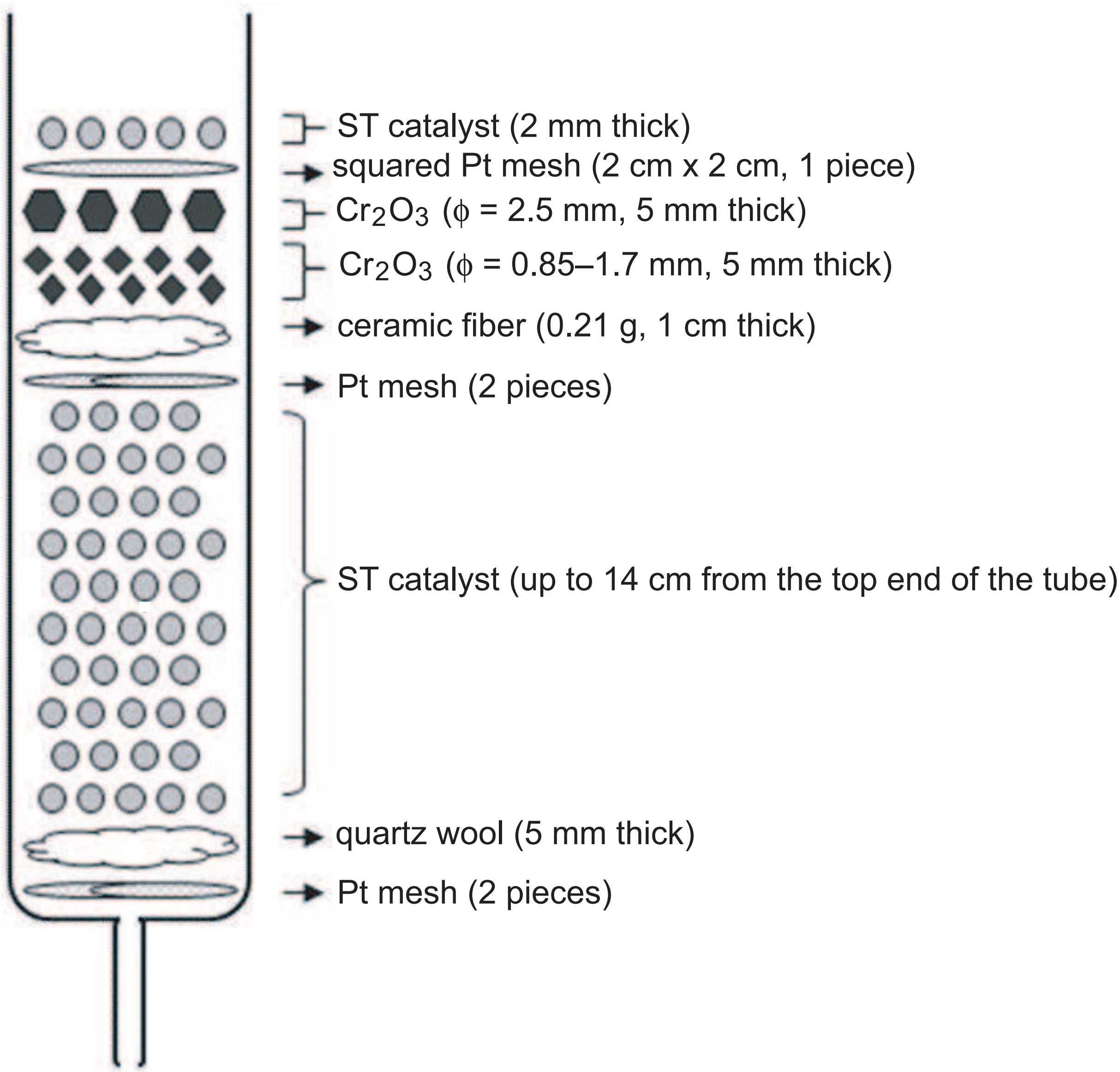

ST catalyst (2 mm thick)
squared Pt mesh (2 cm x 2 cm, 1 piece)
Cr_2O_3 (ϕ = 2.5 mm, 5 mm thick)
Cr_2O_3 (ϕ = 0.85–1.7 mm, 5 mm thick)
ceramic fiber (0.21 g, 1 cm thick)
Pt mesh (2 pieces)
ST catalyst (up to 14 cm from the top end of the tube)
quartz wool (5 mm thick)
Pt mesh (2 pieces)

Fig. 2

Fig S2

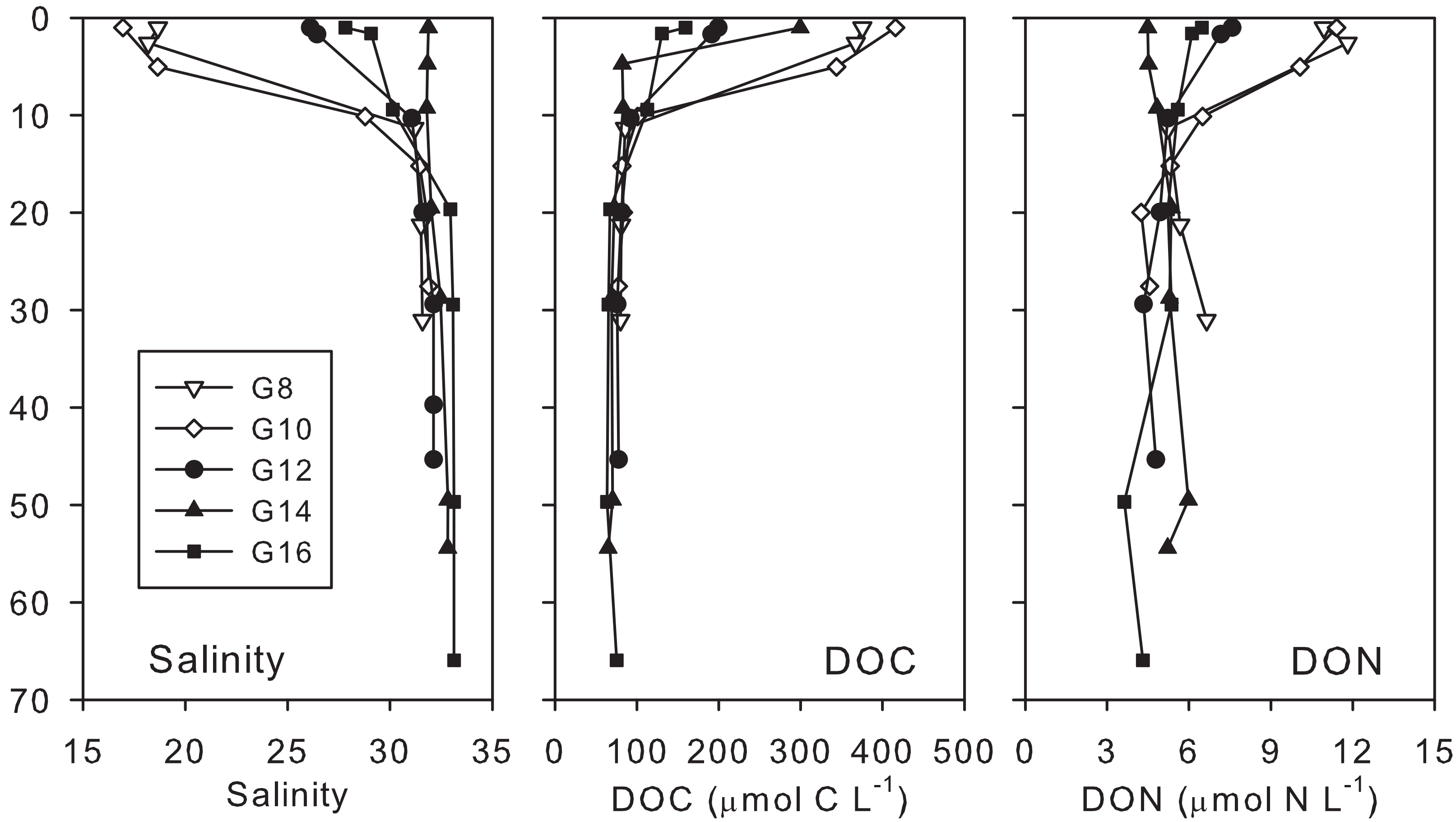

Salinity
G8
G10
G12
G14
G16
DOC
DON
0
10
20
30
40
50
60
70
15
20
25
30
35
0
100
200
300
400
500
0
3
6
9
12
15
Salinity
DOC (μmol C L-1)
DON (μmol N L-1)

Fig S3

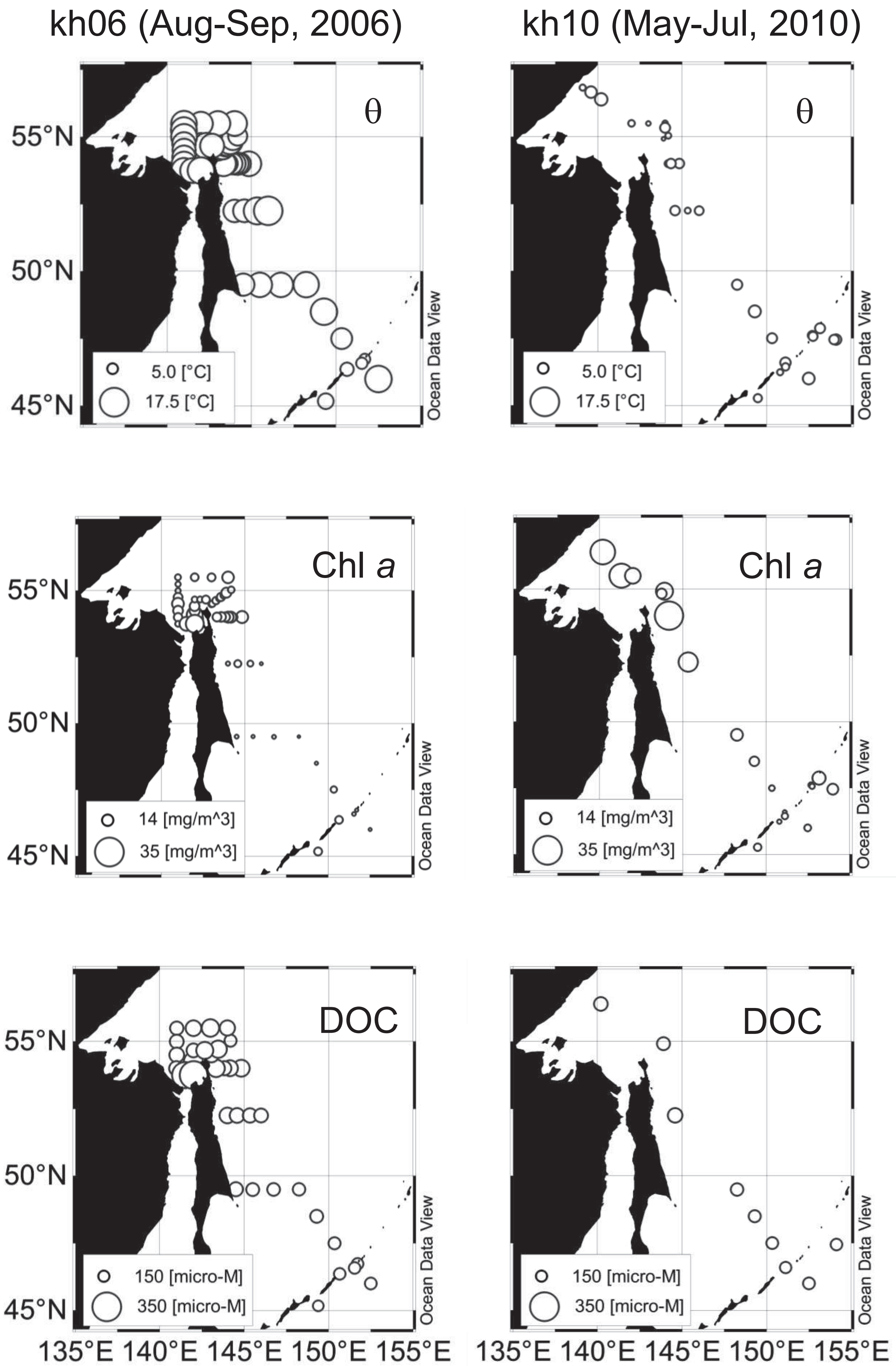

kh06 (Aug-Sep, 2006)
kh10 (May-Jul, 2010)
θ
5.0 [°C]
17.5 [°C]
Chl a
14 [mg/m^3]
35 [mg/m^3]
DOC
150 [micro-M]
350 [micro-M]
55°N
50°N
45°N
135°E 140°E 145°E 150°E 155°E
Ocean Data View